ROYAL .... BEDFORD.

MINISTRY OF TECHNOLOGY

AERONAUTICAL RESEARCH COUNCIL

CURREN J PAPERS

The Performance of an Aerofoil in Stationary and Rotating Cascades

By

E. C. Deverson, H. Marsh

and

J. J. B. Oxford

Performance of an Aerofoil in Stationary and Rotating Cascades

by

E. C. Deverson
H. Marsh
and J. T. B. Oxford.

Summary

A series of experiments have been performed with a rotating cascade wind tunnel to determine the effect of a rotational flow on the behaviour of the blades in a turbomachine. A two-bladed rotor has been tested as a stationary annular cascade- and also when rotating synchronously with a solid body rotational flow. It is then possible to make a direct comparison between the behaviour of the same blade in irrotational and rotational flows. It is shown that if the level of turbulence is greater than some critical value, then there is no significant difference in the unstalled performance of the blades in the stationary and rotating cascades. However, even at a relatively high level of turbulence, there is a marked difference in the manner in which the blade stalls for the stationary and rotating cascades.

Contents

1.0 Introduction

A series of experiments have been carried out with station-
ary and rotating cascades to determine the effect of a low speed
rotational flow on the behaviour of the blades in a turbomachine.
A simple two-bladed rotor with uncambered aerofoils has been
tested over a range of stagger angles as a stationary annular
cascade and also when rotating synchronously with a solid body
rotational flow (constant axial velocity and circumferential
velocity proportional to radius). By measuring the pressure
distribution around the aerofoil, it is then possible to compare
the behaviour of the same blade in both stationary and rotating
cascades. The two-bladed rotor can be regarded as a ducted
propeller or a simple annular cascade which rotates.

The experimental programme was originally based on the theory
developed by Hawthorne (1) for the effect of a rotational flow on
the lift of an aerofoil of infinite span. Hawthorne considered
the flow past an infinite aerofoil which rotates synchronously
with an unbounded solid body rotational flow. The analysis indi-
cated that when compared with a stationary cascade, there would
be a substantial reduction of lift on the blades in the solid
body rotation flow. The experiments were designed to check this
theory and it was estimated that the blades in the rotating
cascade would produce 17% less lift than in the stationary
cascade. This reduction in lift on the rotating blades could be
detected by measuring the pressure distribution around a blade at
the mid-span position.

In addition to checking the analysis for a rotational flow

past an aerofoil, these experiments have a more fundamental
interest for the design engineer in that it has been possible to
make a direct comparison of the behaviour of the same blade in
both a stationary and a rotating cascade. The performance of a
section of a rotor blade is usually compared with the performance
of the same blade section in a stationary linear cascade, an
approach which neglects the influence of neighbouring blade sec-
tions,in particular the blade twist and the variation of lift
along the span of the blade. A direct comparison of the perfor-
mance of the blade in stationary and rotating cascades is diffi-
cult to obtain and in these experiments, this was achieved by the
use of a solid body rotation flow. The same blades have been used
in both the stationary and the rotating cascades and relative to
the blade row, the inlet flow conditions are identical. It is
therefore possible to make a direct comparison of the behaviour
of the two cascades.

2.0 The Theoretical Basis for the Experiments

The theory for the flow of a rotating fluid over a rotating
aerofoil of infinite span has been given by Hawthorne [1] and
this theory has been extended by Denton [2] to the flow of a
rotating fluid past a rotating cascade in an annulus. The work
of Hawthorne and Denton forms the basis for these experiments and
a review of their analysis may help to explain certain unusual
features in the design of the apparatus.

The equation of motion for the fluid in a co-ordinate system
which rotates with the cascade is

$$\frac{\partial W}{\partial t} + (\overline{W}.\nabla)\overline{W} + 2\overline{\Omega} \times \overline{W} + \overline{\Omega} \times (\overline{\Omega} \times \overline{r}) = -\frac{1}{\rho} \nabla_p \qquad (1)$$

where $\overline{W}$ is the relative velocity vector and $\overline{\Omega}$ the angular velocity vector of the cascade. For an incompressible flow which is steady relative to the co-ordinary system, this equation reduces to

$$\overline{W} \times (\nabla \times \overline{W} + 2\overline{\Omega}) = \nabla\left(\frac{p_0'}{\rho}\right) \tag{2}$$

where

$$\frac{p_0'}{P} = \frac{p}{P} - \frac{1}{2}\,\Omega^2 r^2 t\frac{1}{2}\overline{W}.\overline{W}$$

The pressure p_0' is the stagnation pressure in the presence of the radial force field of the rotating co-ordinate system. From equation (2), it follows that

$$W.\nabla\left(\frac{\cdot_0}{\cdot}\right) = 0$$

so that $\left(\frac{\smallsmile}{\smallsmile}\right)$ remains constant along the streamlines. For a solid body rotation flow, $\left(\frac{p_0'}{\rho}\right)$ is uniform far upstream, so that $\left(\frac{\smallsmile}{\smallsmile}\right)$ is constant throughout the entire flow. Equation (2) then becomes

$$\overline{W} \times (\overline{\nabla} \times \overline{W} + 2\overline{\Omega}) = 0$$

which has the solution

$$\nabla \times \overline{W} + 2\overline{\Omega} = \lambda\overline{W} \tag{3}$$

where λ is a scalar function. By taking the divergence of this equation and applying the equation of continuity, $\nabla.\overline{W} = 0$, Hawthorne has .&-i&n that λ remains constant along the streamlines. It follows that for the solid body rotation flow, λ can be eval-uated far upstream where $V \times \overline{W} = 0$,

$$\lambda = \frac{2\Omega}{U} \tag{4}$$

where U is the uniform axial velocity of the flow approaching the cascade. If the-rotating cascade produces a velocity perturbation w-where

$$\overline{W} = iU + \overline{w}$$

then equation (3) can be written as

$$\nabla^2 \bar{w} = \lambda^2 \bar{w} = 0 \tag{5}$$

The equation governing the flow through a cascade which rotates synchronously with a solid body rotation flow therefore differs from that which governs the flow through a stationary cascade,

a) $\nabla^2 \bar{w} = 0$ stationary cascade

b) $\nabla^2 \bar{w} \pm \lambda^2 \bar{w} = 0$ rotating cascade.

The difference between the flow in the two cascades is governed by the parameter λ, or in a non-dimensional form Xc, where c is the blade chord.

In Hawthorne's original paper it was assumed that the aerofoil was of infinite span and that the flow did not vary along the span of the blade. It was then possible to obtain an approximate solution for the flow past a flat plate aerofoil and it was shown that the blades in the rotating two-bladed cascade would produce less lift than in the stationary cascade. The experiments were intended to test this theory and for the chosen value of Xc, 0.36, the reduction in lift on the rotating blades was estimated to be about 17%.

Denton (2) has extended the basic theory to the flow of a rotating fluid past a rotating cascade. By restricting the flow along the span of the blade, the annulus walls reduce the effect of rotation on the lift of the aerofoil. Whereas the original theory indicated that standing waves would occur in the flow past an aerofoil of infinite span for all values of Ac, the theory for flow in an annulus shows that these standing waves will not be

dependent on the hub to tip ratio of the annulus. The apparatus used in these experiments has a hub to tip ratio of 0.4 and for $\lambda c = 0.36$, Denton's analysis predicts that standing waves will not occur and that the lift at the mid-span section of the rotating blades will be only 2% less than that in the stationary cascade. The experiments should therefore lead to almost identical pressure distributions around the blade for the rotating and stationary cascades. The theory predicts that the effect of rotation should be very small for $\lambda c = 0.36$, but this effect will increase as λc is increased and standing waves will occur when λc -1.1.

3.0 Apparatus - The Rotating Cascade Wind Tunnel

The main apparatus used in these experiments was the rotating cascade wind tunnel at the Department of Engineering, Cambridge University. A detailed description of this wind tunnel is given in reference (3). The overall design of the tunnel is shown in Figures 1 and 2 for the rotating and stationary cascade tests respectively. A fibre-glass inlet of large diameter leads to the tunnel working section which is of 2 ft. inner diameter and 5 ft. outer diameter, a hub to tip ratio of 0.4. The apparatus has two independent rotors; only the research rotor is shown in Figures 1 and 2, but far downstream, there is the auxiliary fan with variable pitch blading. This design gives the apparatus great flexibility, since the flow conditions can be varied independently of the research rotor. The same tunnel can be used for experiments with stationary and rotating cascades. The research rotor and the auxiliary fan are each driven by a 65 h.p.

variable speed electric motor and the speed of the rotors can be
maintained constant to within ± 0.2%, provided that there are no
gross fluctuations in the supply voltage.

Within the tunnel working section, there are a total of ten
positions in three axial planes for mounting a probe traversing
mechanism. No provision was made in these experiments for circum-
ferential traversing of the probes and only radial traverses
could be made at these ten positions. The probes used in the
tests were a three-hole cantilevered cylinder to measure the
stagnation pressure and angle of yaw and a separate probe for
measuring the static pressure. These two instruments were cali-
brated by comparison with an N.P.L. standard round-nosed pitot-
static probe and a reversible claw type of yawmeter in a new
instrument calibration duct (3).

In order to determine the angular velocity of the solid body
rotation flow, it was necessary to obtain an accurate circumferen-
tial average for the angular velocity. Since the tunnel was not
equipped for circumferential traversing, the average value of the
angular velocity was measured by mounting a cantilevered cylinder
type of yawmeter on the research rotor and rotating this probe.
When the rotating yawmeter was balanced, then the rotational speed
of the rotor was equal to the mean angular velocity of the solid
body rotation flow. This probe measures the average angular velo-
city of the solid body rotation flow as seen by an observer on the
rotating cascade. It is then possible to set the angular velocity
of the rotor such that the inlet flow relative to the rotating
blades is purely axial.

The aerofoil chosen for these experiments was an uncambered
section of 12% thickness to chord ratio and a chord of 6 in., the
profile being NACA 0012. The research rotor had two blades of 18
inches span manufactured from light alloy and these blades could
be set at staggeranglesin the range 0° to $17^\circ 10'$, as shown in
Figure 3. In the stationary cascade, the blades have an inlet
flow which is axial and they produce a swirl in the outlet flow,
there being a reduction in pressure across the cascade. The
blades in the rotating cascade are therefore set to operate as
turbine blades, so that there is again a decrease of pressure
across the blade row.

In one blade there were 28 hypodermic tubes each leading to
a 0.020 in. diameter static pressure hole drilled at the mid-span
section of the blade. The pressure distribution around the blade
was measured by transmitting the pressures through a rotating
pressure transfer unit to a stationary multi-tube manometer. The
pressure transfer device was constructed from standard sealed
ball journal bearings, there being two sealing elements between
adjacent pressure channels. The pressure transfer device con-
tained only sixteen channels; of these,two channels were connected
to the rotating yawmeter and the other fourteen could be connected
to measure the pressure distribution either on the suction sur-
face or on the pressure surface of the blade by means of a
doubling unit,

The apparatus was designed to produce a solid body rotation
flow with an axial velocity of 32.7 ft/sec., the corresponding
Reynolds number for the research blade being 103,000,based on the

blade chord. The critical Reynolds number for the NACA 0012 profile is estimated to be about 800,000 in a low turbulence flow. A transition device consisting of a strip of thickness 0.014 in. with protuberances 0.014 in. high by 0.015 in. wide and 0.187 in. pitch was therefore placed on each blade surface at 12.5% of the chord from the leading edge. It was found that this device was effective in promoting transition at Reynolds numbers above 64,000.

The experiments with the rotating cascade require the production of an accurate solid body rotation flow. This was achieved by the use of radially varying gauzes and a row of inlet guide vanes, as shown in Figure 1. The guide vanes were manufactured from epoxy resin with fibre-glass reinforcement and the radially varying gauzes were constructed by superposition. The flow in the tunnel is initially axial and it then passes through the gauzes and guide vanes which produce a solid body rotation flow in radial equilibrium. It was thought that the flow might separate from the hub, as reported by Bammert and Klaeukens (4), and to prevent this, a complementary set of radially varying gauzes was positioned downstream to reduce the swirl and remove the radial variation of stagnation pressure. No separation of the flow from the hub was observed in the experiments.

For the tests with the stationary cascade, the two sets of gauzes and the inlet guide vanes were removed and the research rotor held stationary, as shown in Figure 2. It was found that there was a small difference between the pressure distributions

that this might be the effect of either rotation or the different levels of turbulence in the two experiments. Two further series of experiments were therefore carried out with the stationary cascade at increasing levels of turbulence. The higher levels of turbulence were obtained by inserting a gauze and a perforated plate.18 in. upstream of the research blades.

3.1 The Effect of Leaks in the Pressure Transfer Device

The pressure transfer device was constructed from sealed ball journal bearings having a synthetic rubber seal reinforced with a steel pressing. In the development of this unit, it was found that the leakage rate was less than 0.1 cc per hour at differential pressures 0 to 14 inches of water and rotational speeds **60** to 800 r.p.m. Further tests were developed to show the effect of leakage on the pressures measured on the rotating blades.

To determine the effect of leakage on the accuracy of pressure measurement, the system of pressure transmission is considered to be a length of hypodermic tubing connecting to a relatively large volume representing the pressure transfer unit and a relatively large bore tube which transmits the pressure back to the multi-tube manometer. The leak is represented by a narrow bore tube leading from the transfer unit, as shown in Figure 4. It is assumed'that all flows are laminar and that the temperature of the air within the system remains constant. The volume of air within the complete pressure line is

$$V = V_o + A(p - p_a)$$

where A is a constant determined by the manometer, For small variations of pressure, $p = p_a + p_1$, the mass flow rate into the

system is

$$\frac{dm}{dt} \approx \left(\frac{V_o + Ap_a}{RT}\right) \frac{dp_1}{dt}$$

But for isothermal laminar flow, the mass flow rate is proportional to the pressure difference, so that if a pressure $p_a + p_o$ is applied to the end of the pressure line and if the transfer device leaks to the ambient pressure p_a, then

$$\frac{dm}{dt} = \alpha(p_o - p_1) - \beta p_1$$

or

$$\frac{dp_1}{dt} = \lambda(p_o - p_1) - \mu p_1$$

where λ and μ are constants determined by the hypodermic tubing and leak respectively. The pressure indicated on the manometer is then

$$P1 = \frac{\lambda p_o}{\lambda + \mu} + Be^{-(\lambda + \mu)t}$$

where B is a constant.

The constant μ was measured by sealing the end of the hypo-dermic tube, applying a small pressure and measuring the time con-stant as this pressure decayed due to leakage. The combined con-stant $(\lambda + \mu)$ was determined by sealing the end of the hypodermic tube, applying a small pressure, opening the end of the tube and measuring the time constant as the pressure decayed. These two tests were carried out over the same range of applied pressure and with the same manometer inclination, so that the constant 'A' remained unchanged. It was found that when operating under the conditions used in these experiments, the applied pressure decayed exponentially and time constants were

$$\frac{1}{\lambda + \mu} \approx 10 \text{ sec.}$$

$$\frac{1}{\mu} \approx 7000 \text{ sec. (worst line)}$$

so that $p_1 = \frac{700}{701} p_0 + Be^{-\frac{t}{10}}$

The steady state error introduced by leakage in the pressure
transfer device, or anywhere in the pressure line, is therefore
less than 0.15%, this being the value for the worst line. For
most channels, the steady state error in pressure is less than
0.1%. It is interesting to note that this is an error of 0.15%
of the pressure measured; the percentage error is independent of
the pressure measured. The effect of leakage on the pressure
measured is therefore negligible and it is possible to measure the
pressure distribution around the blade to the same order of
accuracy in both stationary and rotating cascades.

4.0 The Solid Body Rotation Flow

A solid body rotation flow has a constant axial velocity
and a tangential velocity which is proportional to the radius,

$$V_x = u$$

and $V_\theta = \Omega r$

Ω being the angular velocity of the flow in the r, θ, x co-ordin-
ate system. If this flow is in radial equilibrium, then the
radial variations of static and stagnation pressure in a station-
ary co-ordinate system are

$$p = A + \frac{1}{2} \rho \Omega^2 r^2$$

and

$$p_0 = A + \rho \Omega^2 r^2 + \frac{1}{2} \rho U^2$$

where A is a constant. If the gauzes are arranged so that there

is no loss of stagnation pressure at the outer radius, r_t, then the radial variation of the gauze loss coefficient is

$$\frac{P_{ot} - P_o}{\frac{1}{2} \rho U^2} = \frac{2\Omega^2}{U^2} (r_t^2 - r^2)$$

$$= \frac{(\lambda c)^2}{2c^2} (r_t^2 - r^2)$$

and at the hub, with c $=$ 6 in., r_t $=$ 30 in. and r $=$ 12 in.,

$$\frac{P_{ot} - P_o}{\frac{1}{2} \rho U^2} = 10.5 \, (\lambda c)^2$$

The stagnation pressure loss across the upstream and downstream gauzes is therefore

$$\frac{\Delta P_o}{\frac{1}{2} \rho U^2} = 10.5 \, (\lambda c)^2$$

at all radii, the two gauzes being complementary. The stagnation pressure loss is clearly very high at high values of the parameter λc and the value chosen for these experiments was λc $=$ 0.36. The radial variation of loss coefficient was obtained by superposition of seven gauzes which were then mounted immediately upstream of the inlet guide vanes. The guide vanes had C4 profiles of 10% thickness to chord ratio on a parabolic arc camber line, P40, with a chord of 6 in., the blades being designed to produce an air exit angle corresponding to a solid body rotation flow.

The construction of the gauzes proved to be extremely difficult and several modifications were necessary before *a* satisfactory solid body rotation flow was obtained. The static and stagnation pressures and yaw angle were measured at a distance 6 in. behind the trailing edge of the guide vanes, the probes

being positioned so that they did not traverse through the wakes
of the guide vanes,   These radial traverses were taken at a
Reynolds number of 103,000 based on the axial velocity at the
mid-span position, this being the Reynolds number for the whole
series of experiments. Due to the method of constructing the
gauzes, there were some local discontinuities in the gradient of
stagnation pressure, but the experiments suggest that it is the
overall gradient which is important rather than the local value.
It is possible that the local variations in the gradient of
stagnation pressure decay with distance downstream, while the
overall gradient is retained.

Figures 5 and 6 show the axial and tangential velocities as
functions of the radius and it is clear that over the central
region of the **annulus,** the flow is a good approximation to a
solid body rotation flow with

$$u = 32.7 \text{ ft./sec.}$$

$$\Omega = 11.9 \text{ rad./sec.}$$

This value for Ω is based on a radial traverse which does not
pass through the wake of a blade, whereas the rotating cascade
passes-through **the wakes** of the guide vanes and therefore
observes a slightly different value for Ω.   The angular **velo-**
city observed from the rotbr can be determined by using the rota-
ting **yawmeter with** no blades on the rotor.   It was found that the
yawmeter was balanced when the rotational speed was 110.4 **r.p.m.,**
corresponding to $\Omega = 11.6$ **rad./sec.** at the standard test conditions
of 29.92 in. Hg. and 60 $^{\circ}$F. The main tests with the rotating
cascade were performed at a rotational speed of 110.4 r.p.m., but

additional results were also obtained at a speed corresponding to the yawmeter being nulled.

5.0 Experiments with the Rotating Cascade

The two-bladed rotor was rotated synchronously with the solid body rotation flow while a constant Reynolds number of 103,000 was maintained, this being based on the axial velocity and the blade chord. The variation of viscosity with temperature. is given by Sutherland's formula,

$$\mu \propto \frac{T^{\frac{3}{2}}}{T+A}$$

where A is a constant. It follows that the axial velocity and the angular velocity must be varied such that,

$$U, \Omega \propto \frac{\mu}{\rho} \quad \propto \frac{T_a^{\frac{5}{2}}}{(T_a+A)p_a}$$

where p_a and T_a are the ambient pressure and temperature. The variations of ambient pressure and temperature are such that the tunnel operating condition and the rotor speed must be continually adjusted to maintain the correct Reynolds number and inlet flow angle relative to the rotating blades. The rotational speed of the **rotor** could be maintained constant to within ± 0.2 r.p.m., this corresponding to a variation of ± 4 minutes in the air inlet angle. The blade stagger angle was set to an accuracy of ± 2 minutes, using an inclinometer on a machined face, so that the overall accuracy in incidence due to speed and stagger was about ± 0.1'.

The pressure distribution around the blade at the mid-span

position was measured at stagger angles from $0°$ to $17°10'$ **and** after correcting for, the effect of rotation on the air in the rotating pressure line, the pressure coefficient was calculated,

$$C_p = \frac{p - p'}{\frac{1}{2} \rho U^2}$$

where p' is the static pressure measured at the mid-span position **6** in. upstream of the rotor blade leading edge. The variation of the pressure coefficient with position along the chord is shown in Figures 7 and 8. For clarity, the pressure profile at zero stagger is not shown, but it was found to be almost identical for the two surfaces and the slight difference was probably caused by small errors in the blade profile close to the leading edge. The pressure distributions have been integrated to obtain the lift coefficient, C_L, measured normal to the chord line, there being no measure of the drag coefficient so that it was not possible to calculate the lift along the cascade. Figure 9 shows the variation of lift coefficient with stagger angle. There is a gradual change from unstalled to stalled operation as the stagger angle is increased beyond $12°30'$; a region of separated flow develops from close to the leading edge and the point of re-attachment moves back along the blade as the stagger angle is increased. It is doubtful whether a steady re-attachment occurs at stagger angles greater than $15°$, but there is still a **sub**-stantial rise in pressure along the suction surface for $\xi = 17°10'$. This is the thin-aerofoil type of stall described by Crabtree (6) in which a 'long bubble' forms and grows with increasing incidence until eventually, the separated layer fails to re-attach to the aerofoil surface.

A hot wire anemometer was used to determine the longitudinal component of the main stream turbulence at a position 6 in. upstream of the rotor blade leading edge and it was found that at the mid-span position, the turbulence level(T.L. in the diagrams) was 1.75%. This is the turbulence level for the main stream flow outside of the wakes of the inlet guide vanes. The effective turbulence level for the rotor will be higher than 1.75% because of the rotor passing through the wakes of the inlet guide vanes.

5.1 The Behaviour of the Rotating Yawmeter

The main purpose of the rotating yawmeter was to determine the average angular velocity of the solid body rotation flow without the blades mounted on the rotor. However, it had been suggested that this yawmeter could be used with the blades mounted on the rotor in order to determine the synchronous speed and thereby set the inlet air angle for the rotating cascade. A few preliminary tests showed that the speed required to balance the yawmeter was dependent on the stagger angle of the blades. Furthermore, even with the blades set at zero stagger, the speed to null the yawmeter, 111.4 r.p.m., was not the same as that obtained when there were no blades on the rotor, 110.4 r.p.m. There was therefore some doubt concerning the correct rotational speed for the experiments and it was essential to find the reason for this unusual behaviour.

In order to estimate the effect of blade stagger on the behaviour of the rotating yawmeter, the two blades spanning the annulus are considered as part of an infinite flat plate propeller

and the effect of flow along the span is neglected. The math-
matical model is shown in Figure 10, the angle of attack of the
flat plate being ξ for $r > 0$ and $-\xi$ for $r < 0$. The rotating yaw-
meter is assumed to lie in the same axial plane as the bound
vorticity of the blades. The propeller forms a flat plate aero-
foil with a step change in the angle of attack at $r = 0$ and the
circulation around the aerofoil at any radius r can be expressed
as

$$\frac{\Gamma(r)}{\pi c U \xi} = \frac{2}{\pi} \int_0^\infty \frac{\sin(wr)}{w(1 + \frac{\pi c w}{4})} dw$$

so that the trailing vorticity is

$$\frac{1}{\pi c U \xi} \frac{d\Gamma}{dr} = \frac{2}{\pi} \int_0^\infty \frac{\cos(wr)}{(1 + \frac{\pi c w}{4})} dw$$

The induced tangential velocity at the probe head P is then

$$V_\theta = \frac{1}{2\pi} \int_0^\infty \frac{R^2}{R^2 + r^2} \frac{d\Gamma}{dr} dr$$

$$= -\frac{2U\xi}{\pi} e^{\frac{4R}{\pi c}} Ei^{(-\frac{4R}{\pi c})}$$

where $- Ei(-x) = \int_x^\infty \frac{e^{-t}}{t} dt.$

This integral has been tabulated by Jahnke and Emde(5) and for
R = 21 in., c = 6 in. the induced flow angle is

$$\frac{V_\theta}{U} = 0.125$$

To balance the rotating yawmeter, it is necessary to reduce the
rotational speed below that of the solid body rotation flow

$$\Delta N = - 0.37\xi \quad r.p.m.$$

where ξ is measured in degrees.

This simple theory explains why the speed to balance the yaw-

meter is dependent on the blade stagger angle, but it does not explain the increase in speed required to balance the **yawmeter** when the stagger angle is zero. However, at the inner and outer walls of the **annulus,** there are boundary layers and the flow is no longer a good approximation to a solid body rotation flow. At the hub and tip sections of the blades, there is a large negative incidence and this produces an induced flow at the probe which is in the opposite direction to that caused by the blade stagger. The effect of the boundary layers is that an increase of speed, 6, is required in order to balance the yawmeter. The magnitude of this increase in rotational speed cannot be esti-mated without more detailed information about the performance of the blades at high negative incidence in a shear flow.

From these arguments, it follows that the rotational speed to null the **yawmeter** is

$$N_{null} = 110.4 \text{ t } \delta - 0.37\xi \text{ r.p.m.}$$

and the experiments showed that δ was 1.0 r.p.m. The speed to balance the **yawmeter** is compared with the theoretical value in Figure 11. There is close agreement with the theory for stagger angles less than 10°, but for higher stagger angles, there is little change in the speed at which the **yawmeter** is balanced. This is probably the result of regions of stall at the blade hub and tip extending towards the mid-span position as the stagger angle is increased.

The lifting line model for the flat plate propeller at a small stagger angle can also be used to estimate the lift on the blades at the mid-span section. The equation for the radial vari-ation of circulation can be integrated to give

$$\frac{\Gamma(r)}{\pi c U \xi} = 1 + \frac{2}{\pi} \{ \cos(\frac{4r}{\pi c}) [Si (\frac{4r}{\pi c}) - \frac{\pi}{2}] - \sin (\frac{4r}{\pi c}) Ci (\frac{4r}{\pi c}) \}$$

where

$$Si(y) = \frac{\pi}{2} - \int_Y^\infty \frac{Sint}{t} dt$$

and

$$Ci(y) = \int_Y^\infty \frac{cost}{t} dt .$$

These integrals have also been tabulated by Jahnke and Emde (5).
At the mid-span section, the circulation is

$$\Gamma = \pi c U \xi$$

so that the lift at this section is 13.2% less than the corres-
ponding value for an isolated flat plate. There is seen to be a
substantial reduction in lift caused by placing the blades in an
annular cascade, even when the cascade contains only two blades.
From this model with flat plates of zero thickness, the lift co-
efficient is estimated to be

$$C_L = 0.095\xi$$

where ξ is measured in degrees. The experimental value for the
blades with 12% thickness to chord ratio is

$$C_L = 0.088\xi$$

which is in fair agreement with the lifting line model.

6.0 Experiments with the Stationary Cascade

Before testing the blades as a stationary cascade, the cir-
cumferential uniformity of the tunnel flow was checked by radial
traverses at four circumferential positions. It was found that
outside of the boundary layers, the axial velocity variation was
± 0.5% and the flow did not deviate from the axial direction by
more than 15 minutes. At the mid-span position, the flow angle

was 9 minutes in a direction to increase the incidence onto the
blade.

The pressure distribution around the blade was measured at
a Reynolds number of 103,000 for stagger angles in the range 0°
to $17^O10'$ and the corresponding pressure coefficients are shown
in Figures 12 and 13.   The variation of the lift coefficient with
stagger angle is compared with that for the rotating cascade in
Figure 14.   There is a small difference between the pressure dis-
tributions for an unstalled blade in the two cascades, the lift
coefficient for the stationary cascade being about 10% greater
than that for the rotating cascade for stagger angles less that
$8^O45'$.   At $\xi = 8^O45'$, a small region of separated flow forms close
to the leading edge and as the stagger angle is increased, the
point of re-attachment moves back along the blade.   When the
stagger angle is increased beyond about $13^O05'$, then the flow can
no longer re-attach itself and the blade stalls with the flow
separating from a point near to the leading edge.   This is similar
to the leading edge stall described by **Crabtree** (6) in which a
'short **bubble**' forms close to the leading edge and when the inci-
dence is increased, this bubble bursts leading to a well-separated
flow and a sudden loss of lift.   **Crabtree** (6) defines a 'short
bubble' as a region of separation which has little effect on the
pressure distribution, while a 'long bubble' has a marked effeot
on the pressure distribution.   With this simple physical criterion
the experiments show that at $\xi = 13^O05'$, there is a 'long bubble'
present on the blade.   The experiments suggest that the blade has

'long bubble' grows very rapidly with increasing incidence, so that there is a rapid reduction in lift.

It was thought that the difference in the unstalled performance might be experimental error, but tests showed that the experimental results were repeatable and no error could be found in the instrumentation or apparatus. This led to the conclusion that the experiments showed either the effect of rotation or the difference in turbulence levels for the two cascades. The longitudinal component of turbulence was found to be 0.25%, whereas the corresponding value for the rotating cascade was estimated to be greater than 1.75%. To distinguish between the effects of rotation and turbulence level, it was decided to test the stationary cascade at higher levels of turbulence,

An open gauze was placed 18 in. upstream of the blade leading edge to raise the level of turbulence. The radial traverses were repeated to check the uniformity of the flow and it was found that outside of the boundary layer, the axial velocity was constant to within ±1% and at the mid-span position, the flow deviated from the axial direction by only 5 minutes, the incidence being increased by this error. The longitudinal component of turbulence was measured at the mid-span position 6 in. before the research blade leading edge and it was found to be 1.35%.

Figures 15 and 16 show the pressure coefficients measured at this higher level of turbulence. It was found that for the unstalled blade, the pressure distributions for the rotating and stationary blades were almost identical. The variation of lift-

coefficient with stagger angle is shown in Figure 17, where it is
compared with that for the tests at a low level of turbulence and
that for the rotating cascade. For the unstalled blade, there is
little difference between the performance of the rotating and
stationary cascades and this is in agreement with the theory
developed by Denton (2) for a solid body rotation flow. The
experimental results show that if the turbulence level is above
some critical value in the range of 0.25% to 1.35%, then for a
hub to tip ratio of 0.4 and $\lambda_c = 0.36$, there is no significant
difference in the unstalled performance of the aerofoil in the
rotating and stationary cascades.

The pressure distributions measured in the stationary cascade
show that with the increased level of turbulence, the formation
of a separation 'bubble' close to the leading edge is delayed
until the stagger angle reaches 10°. Again there is a 'short
bubble' on the blade which becomes a 'long bubble' at $\xi = 13^o 30'$
and this 'long bubble' grows very rapidly with increasing inci-
dence. However, it is clear that there is still a marked differ-
ence in the manner in which the blades stall in the stationary
and rotating cascades. It was therefore decided to repeat the
experiments with the stationary cascade at a higher level of tur-
bulence to try to determine whether this difference in the stal-
ling characteristic was caused by the rotation or the different
levels of turbulence.

For the third series of tests with the stationary cascade,
a perforated metal plate with square holes of side 0.375 in. and
pitch 0.563 in. was placed 18 in. upstream of the research blade

leading edge. The stagnation pressure loss across this plate
was extremely high and the experiment was just within the range
of tunnel operating conditions. The longitudinal component of
turbulence was measured at the mid-span position 6 in. ahead of
the blades and the turbulence level was found to be 3.3%. A
radial traverse at the same position showed that outside of the
boundary layers, the axial velocity varied by ±5% and the apparent
flow angle varied from the axial direction by as much as t 2$^\text{O}$.
The yawmeter may not read correctly in this type of flow and it
was thought that the true flow direction was almost axial. There
was a periodicity in the traverse readings corresponding to the
perforations in the plate; the high turbulence level had been
achieved, but only at the expense of a non-uniformity in the flow.
With these local variations of flow, it was not possible to obtain
accurate pressure distributions around the blade, since the mano-
meter readings varied with the positioning of the blade relative
to the grid. The experiments were therefore limited to a study
of the mode of stall in this highly turbulent flow.

Typical pressure distributions are shown in Figure 18 and
these can be compared with the results obtained at lower levels
of turbulence and also in the rotating cascade. There is good
agreement between the pressure distribution at this high level of
turbulence and that for the rotating cascade at a stagger angle
of 12$^\text{O}$30'. As the stagger angle is increased to 13$^\text{O}$45', the blade
stalls gradually as the region of separated flow develops close
to the leading edge. A further increase in the stagger angle to
14$^\text{O}$20' leads to a substantial reduction in lift on the blade. The
pressure distribution for $\xi = 15^\text{O}$ shows that separation occurs very

close to the leading edge and that this is followed by a rise in
pressure along the suction surface. Figures 13 and 16 show that
this increase in pressure along the suction surface did not occur
at the lower levels of turbulence, but Figure 8 shows that a
greater increase of pressure was observed in the rotating cascade.
The pressure distributions for $= 13^{\circ}45'$, Figure 19, show that
increasing the level of turbulence produces a behaviour at stall
which is in closer agreement with that of the rotating cascade.
These experiments suggest that when the 'long bubble' forms on
the stationary blades, the rate of growth of the bubble with
stagger angle is reduced at the higher levels of turbulence.
Figure 20 shows the variation of lift coefficient with stagger
angle for the complete series of experiments and it can be seen
that as the turbulence level is increased, there is close agree-
ment between the lift coefficients of the stationary and rotating
cascades over a wider range of stagger angles. The results
obtained at the high level of turbulence are far less accurate
than those of the earlier tests.

It is difficult to provide a complete explanation for the
different behaviour of the two cascades at high stagger angles,
but this is probably influenced by the flow along the span of the
blade and the structure of the turbulence. Hawthorne (1) has
shown that one of the features of the flow past a rotating aero-
foil in a solid body rotation flow is the generation of a velocity
along the span of the blade. It is possible that the separation
and re-attachment of the flow close to the leading edge is influ-
enced by this flow along the span. With regard to turbulence, the

important, but it is also possible that the stalling character-
istic of the cascades may be influenced by the structure and
energy spectrum of the turbulence.   In the stationary cascade,
the turbulence may be almost isotropic with a characteristic
length, or scale, and a certain energy spectrum.   In the rotating
cascade, the research blade passes through the wakes of the inlet
guide vanes so that relative to the rotating blades, the turbu-
lence is **no** longer isotropic, the characteristic length may
differ from that of the stationary cascade and the energy spectrum
will have a large peak at a frequency which corresponds to passing
through the wakes of the inlet guide vanes.   In these experiments
it has not been possible to make a detailed study of the effect
of turbulence on the performance of a cascade, but the results
suggest that the effective turbulence level for the rotating
cascade is very high and that the performance of the blades at
high stagger angles is dependent on the turbulence level and may
be influenced by the structure of this turbulence.

7.0 Conclusions

Experiments with the same blade at the same Reynolds number
in the rotating and stationary cascades have shown that provided
that the level of turbulence is above a critical value, then there
is no significant difference in the unstalled performance of the
two cascades.   This is in agreement with the theory developed by
Denton (2) for flow past a rotating cascade of finite span. It
has been found that there is close agreement in the pressure dis-
tributions measured in the two cascades over a wider range of
stagger angles as the turbulence level is increased.   The stagger

angle at which the stationary cascade stalls increases as the turbulence level increases and the stall becomes more gradual. However, even at the highest level of turbulence, 3.3%, the manner in which the stationary blades stalled was not the same as that for the rotating cascade . This difference in the behaviour of the blade at high stagger angles may be caused by flow along the span of the blade, the high effective turbulence level for the rotating cascade or the structure of the turbulence as seen by the stationary and rotating cascades.

8.0 Acknowledgements

The authors-would like to thank the Science Research Council and the Ministry of Aviation who have supported this research project.- Many members of the Engineering Department have contributed to the project by their enthusiasm, interest and practical experience, in particular Professor W. R. Hawthorne, Mr. H. G. Rhoden, Mr. A. Barker and Mr. R. Carter who assisted in many of the experiments.

9.0 References

1. Hawthorne, W. R.   The flow of a rotating fluid over a rotating aerofoil. A.R.C. 27,130, 1965.

2. Denton, J.D.   Standing wave motions in swirling flows. Ph.D. Thesis in preparation Cambridge University.

3. Oxford, J. T. B.   A rotating cascade wind tunnel and a rotating aerofoil in a rotational flow. Ph.D. Thesis, Cambridge University.

4. Bammert, K. and Klaeukens, H.   Nabentotwasser hinter Leiträdern von axialen Strömungsmaschinen. Ing. Arch. 17, 1949.

5. Jahnke, E. and Emde, F.   Tables of Functions, Dover, 1945 edition.

6. Crabtree, L. F.   The Formation of Regions of Separated Flow on Wing Surfaces. A.R.C. R. & M. 3122, 1957.

10. Notation

c	blade chord,
C_L	lift coefficient measured normal to the chord,
C_p	local pressure coefficient,
p	static pressure,
p'	static pressure measured at the mid-span position 6 in. upstream of the research blades,
p_0	stagnation pressure,
p_0'	stagnation pressure in the rotating co-ordinate system,
r	radius,
R	radius of the rotating yawmeter,
t	time,
T.L.	turbulence level,
U	axial velocity,
$\overline{V}$	velocity vector,
$\overline{w}$	relative velocity perturbation,
$\overline{W}$	relative velocity vector,
μ	viscosity,
ρ	density,
ξ	stagger angle,
Ω	angular velocity.
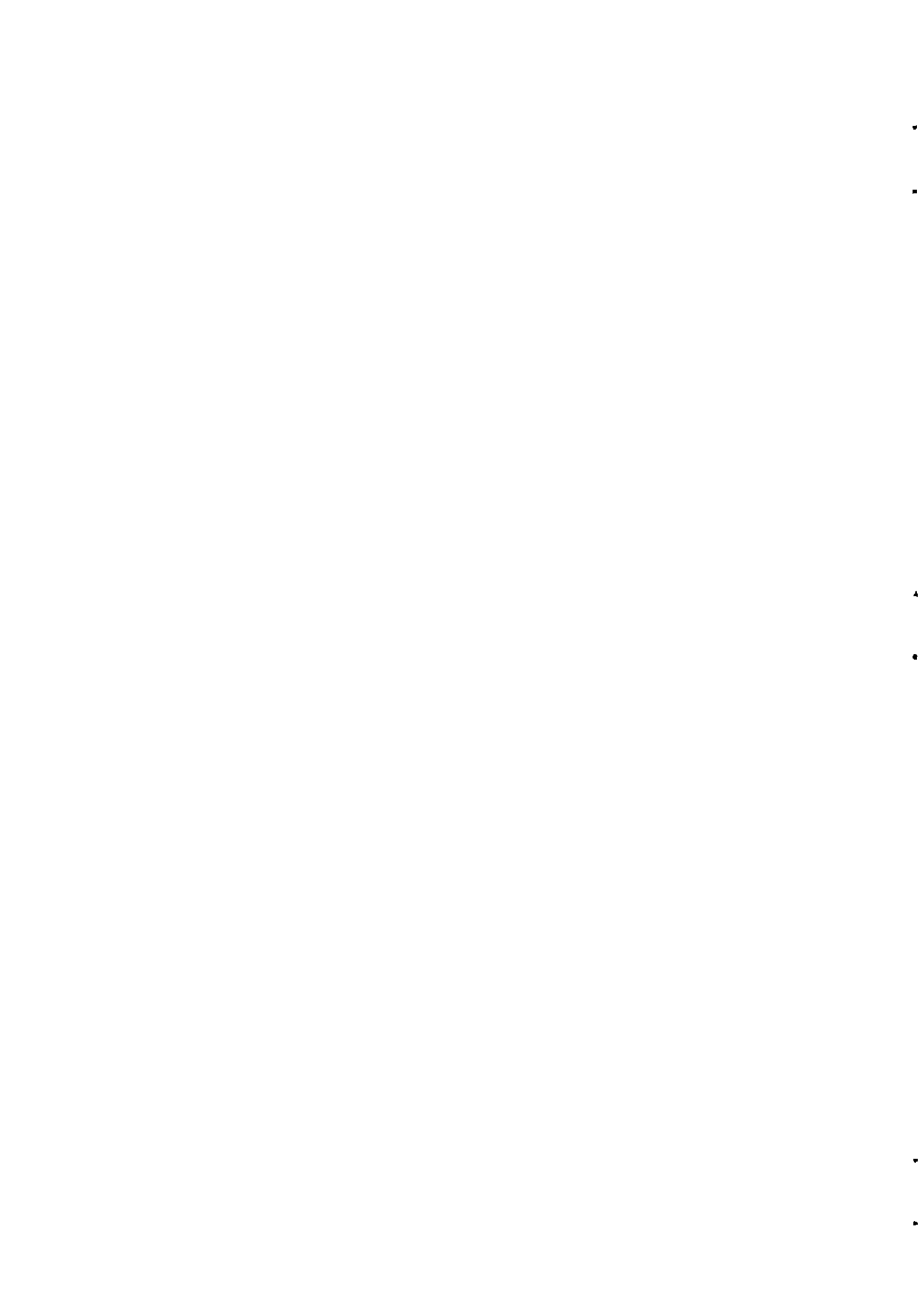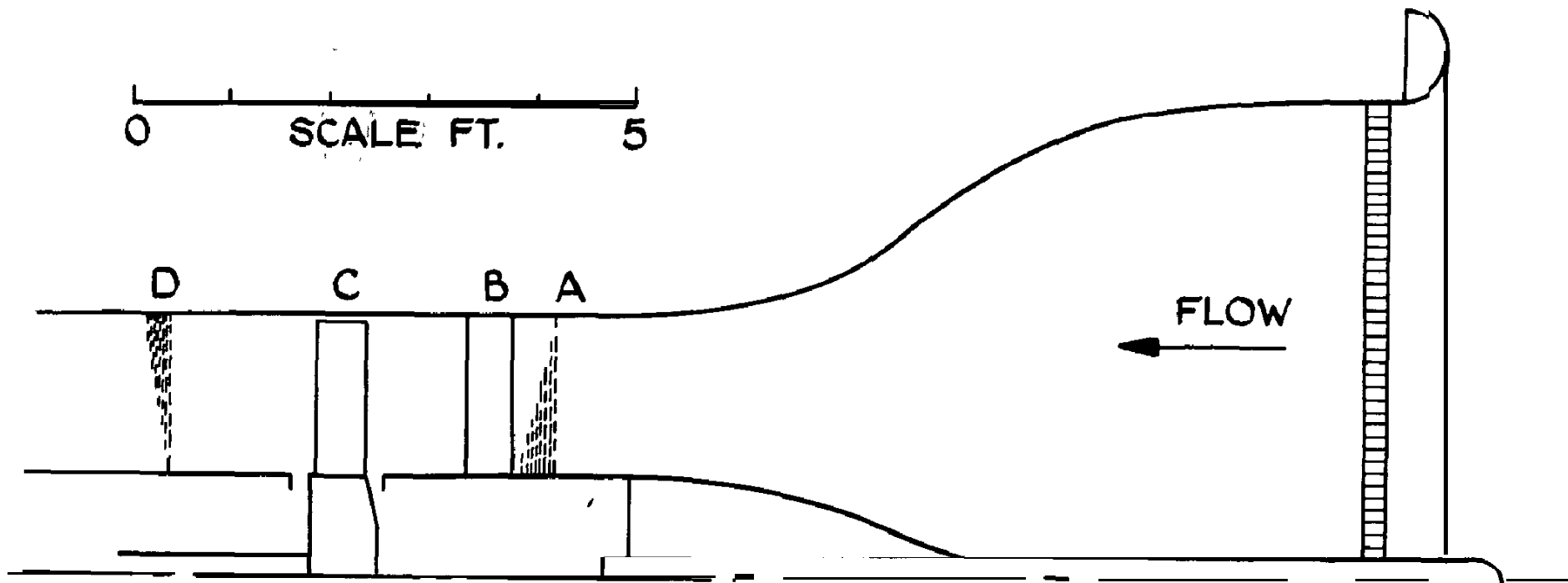
A UPSTREAM GAUZE,   C TWO-BLADED ROTOR,
B   IN LET GUIDE VANES,   D DOWNSTREAM GAUZE.

FIG. 1. OVERALL VIEW OF ROTATING CASCADE.
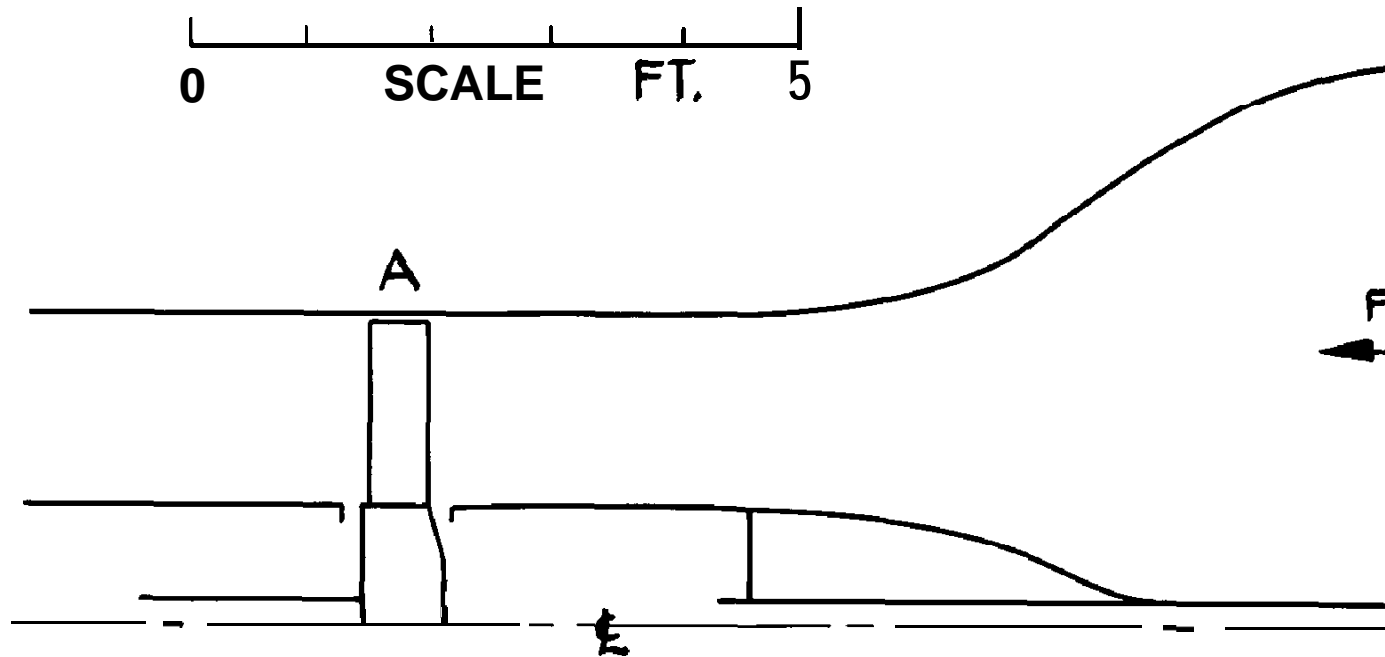
FIG. 2. OVERALL VIEW Of= STATIONARY CASCAC
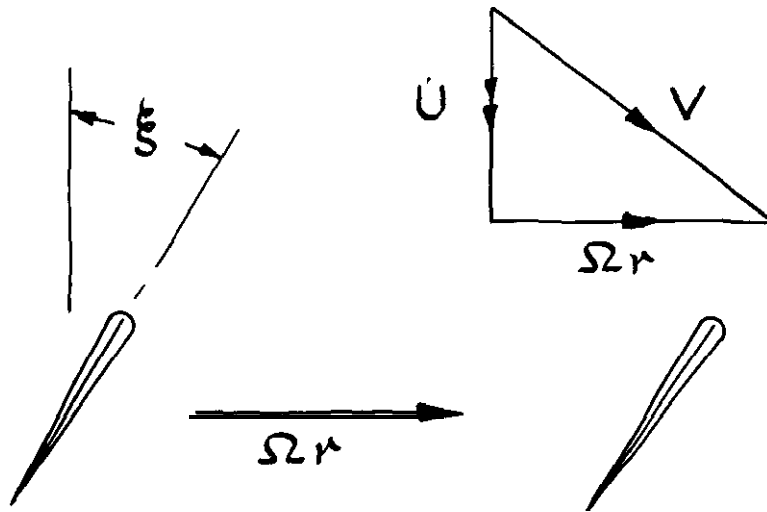
a) ROTATING CASCADE
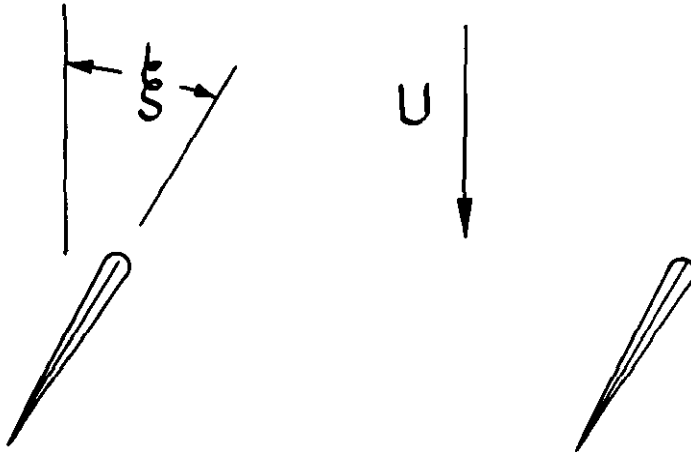
b) STATIONARY CASCADE
VI EW LOOKING RADIALLY OUTWARDS

FIG.3. NOTATION

BLADE TAPPING

TRANSFER UNIT   MANOMETER

a) TRANSFER DEVICE

LEAY

P_a

BLADE TAPPING   Pa

$P_a + P_o$ —————— $P_a + P_1$
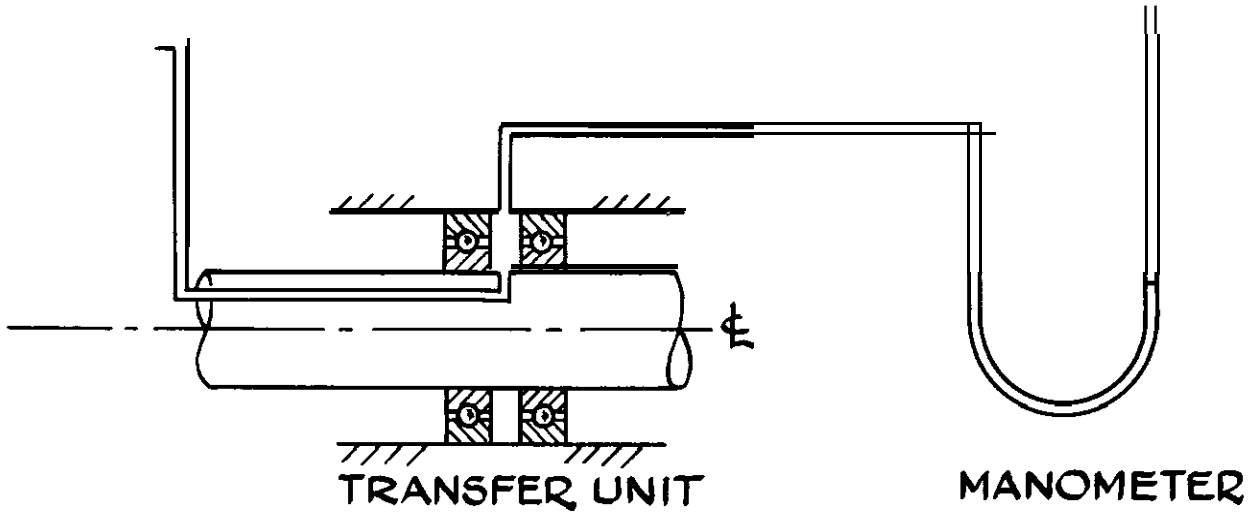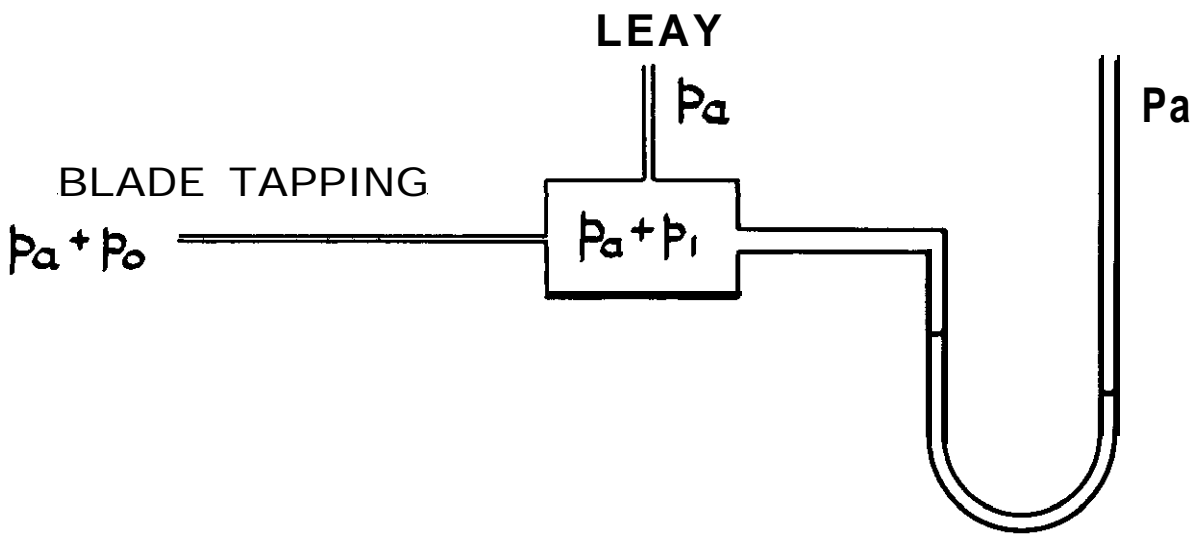
b) MODEL FOR LEAK ANALYSIS

FIG, 4. PRESSURE TRANSFER DEVICE
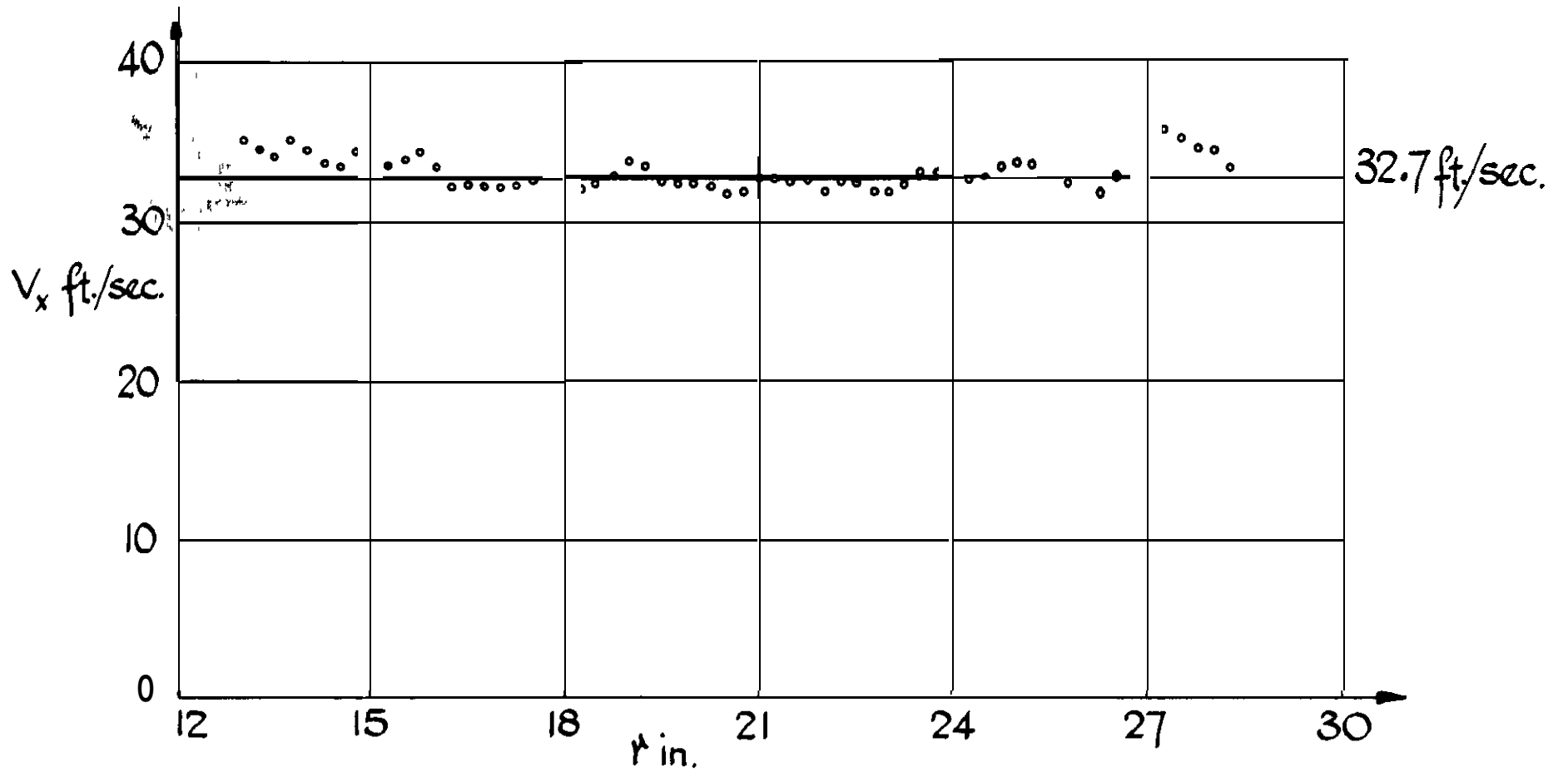
FIG. 5. AXIAL VELOCITY, SOLID BODY ROTATION
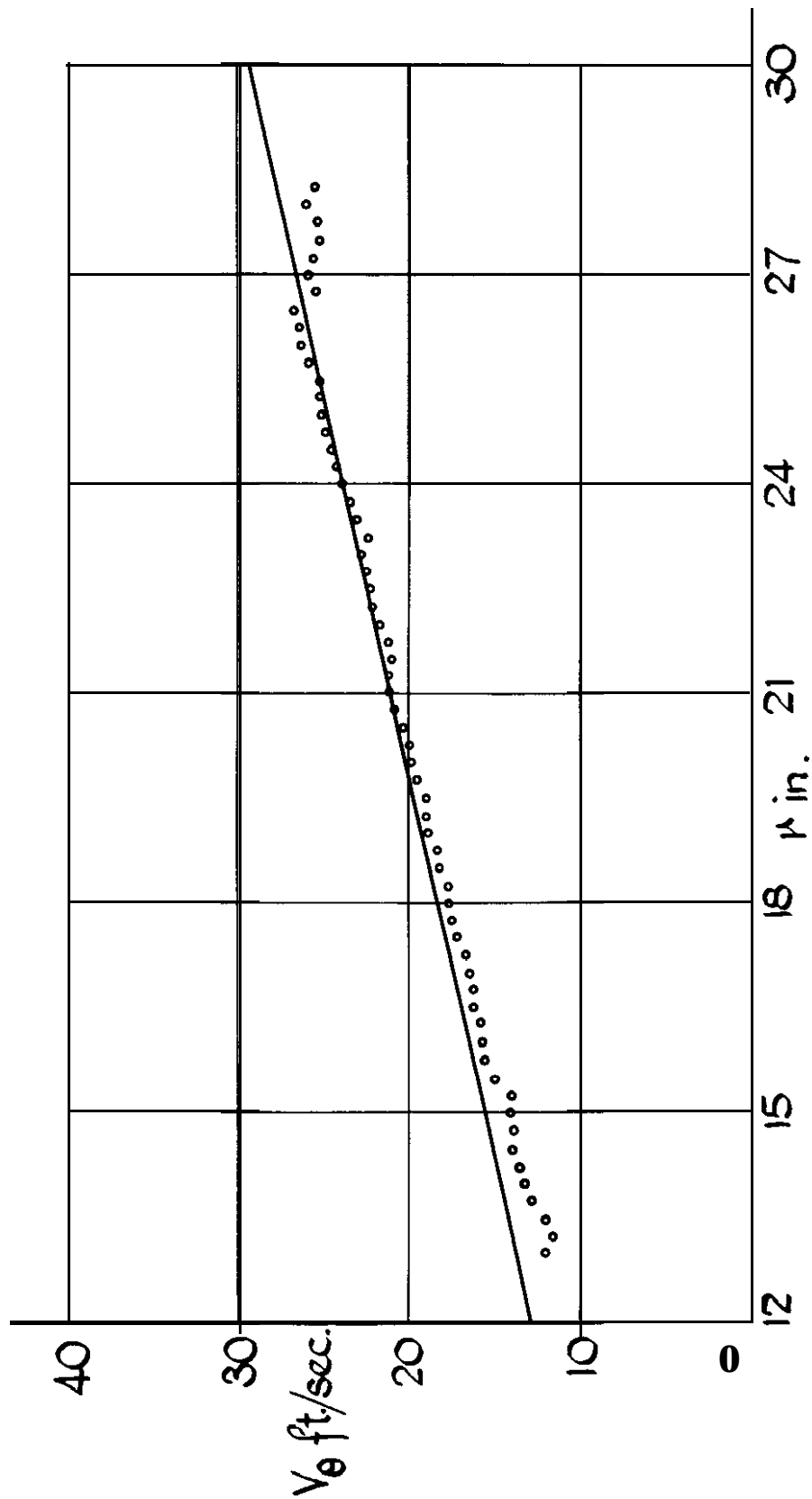
FIG. 6. TANGENTIAL VELOCITY, SOLID BODY ROTATION

$$C_p = \frac{p - p'}{\frac{1}{2}\rho U^2} \qquad Re = 103,000$$

T.L. > 1·75%

● ξ = 5°
○ ξ = 7° 30'
✕ ξ = 10°
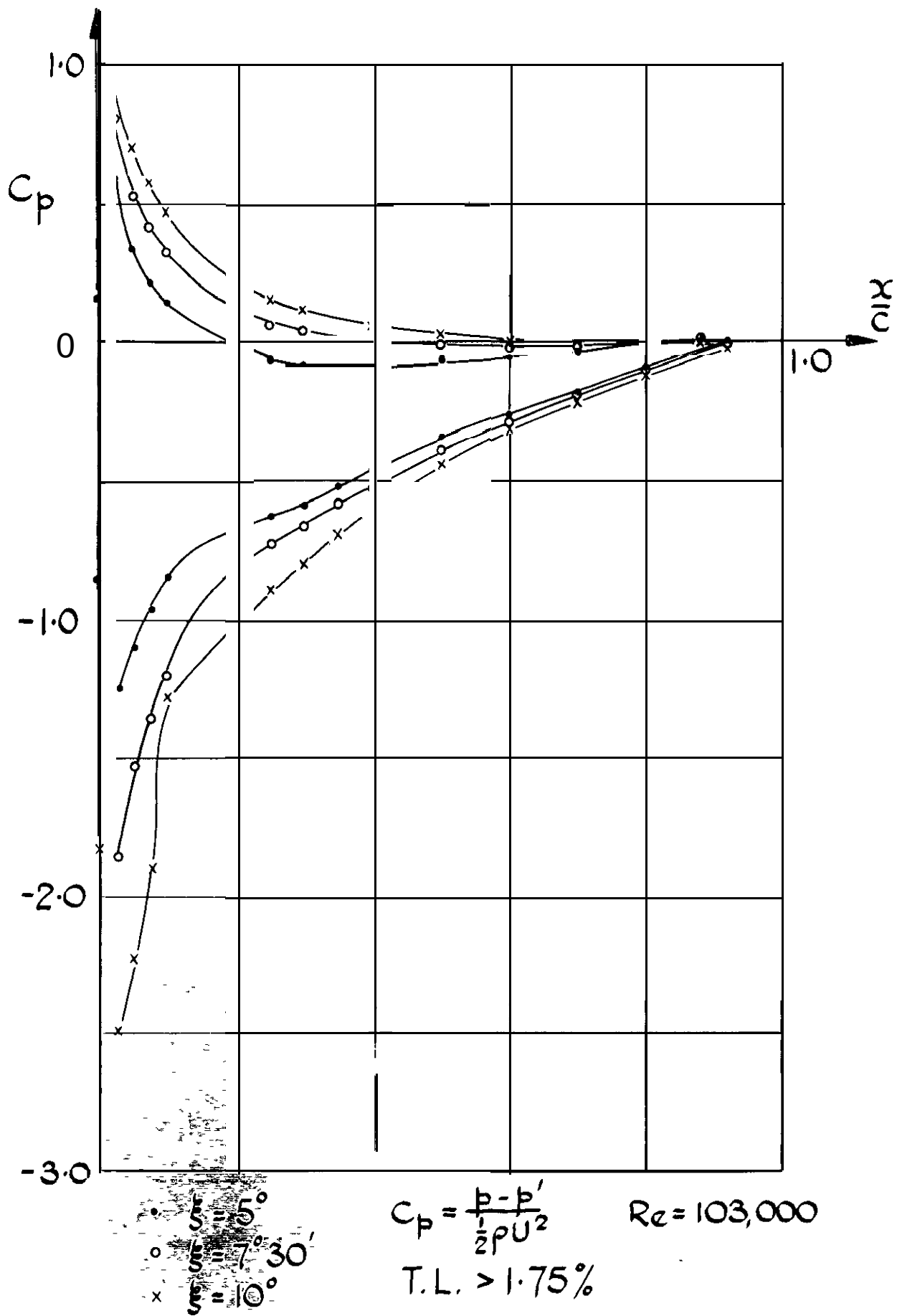
FIG, 7. Cp FOR ROTATING BLADE
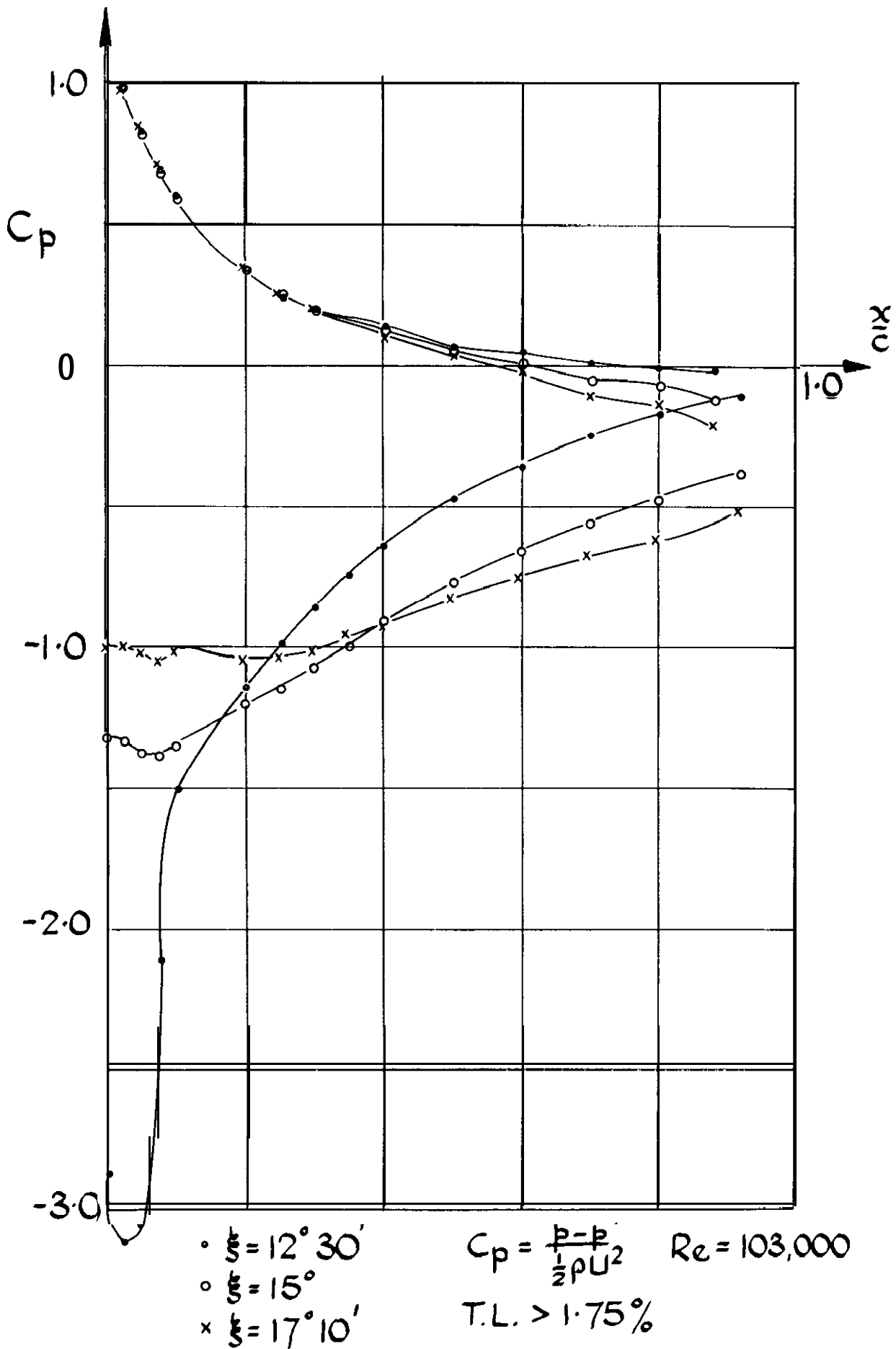
FiG.8. Cp FOR ROTATING BLADE
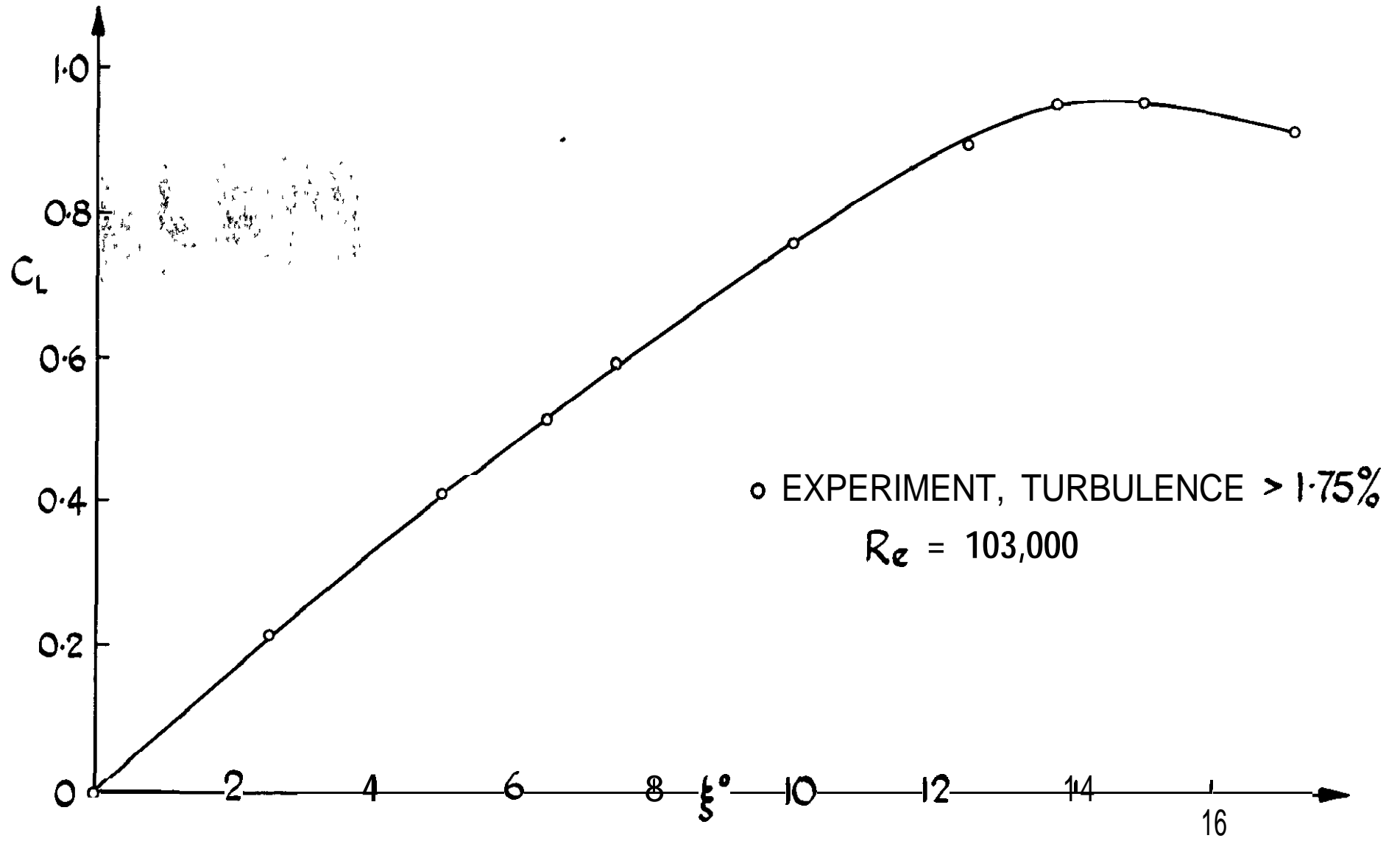
FIG.9. C_L vs ξ ROTATING BLADE
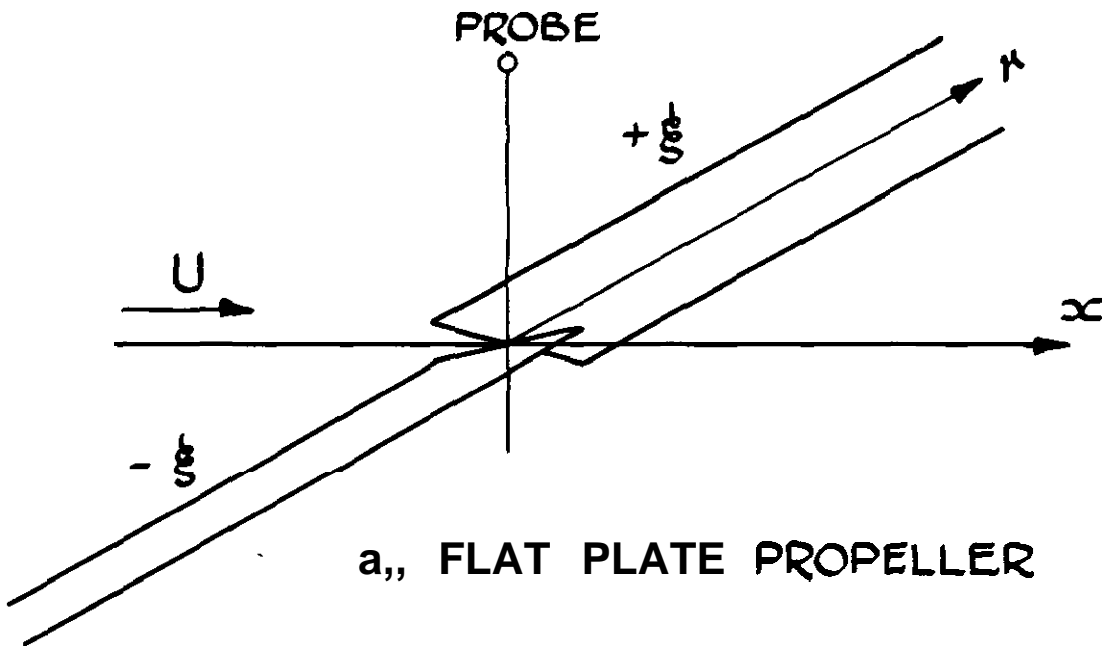
a,, FLAT PLATE PROPELLER
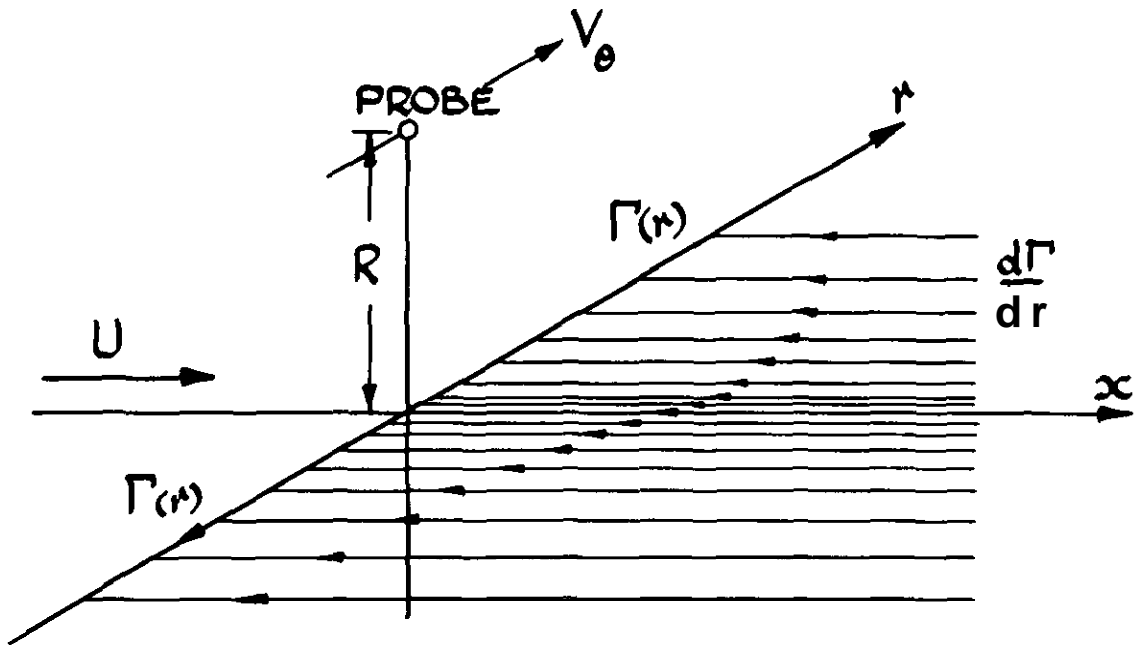
b) LIFTING LINE MODEL

FIG.10. ROTATING YAWMETER.
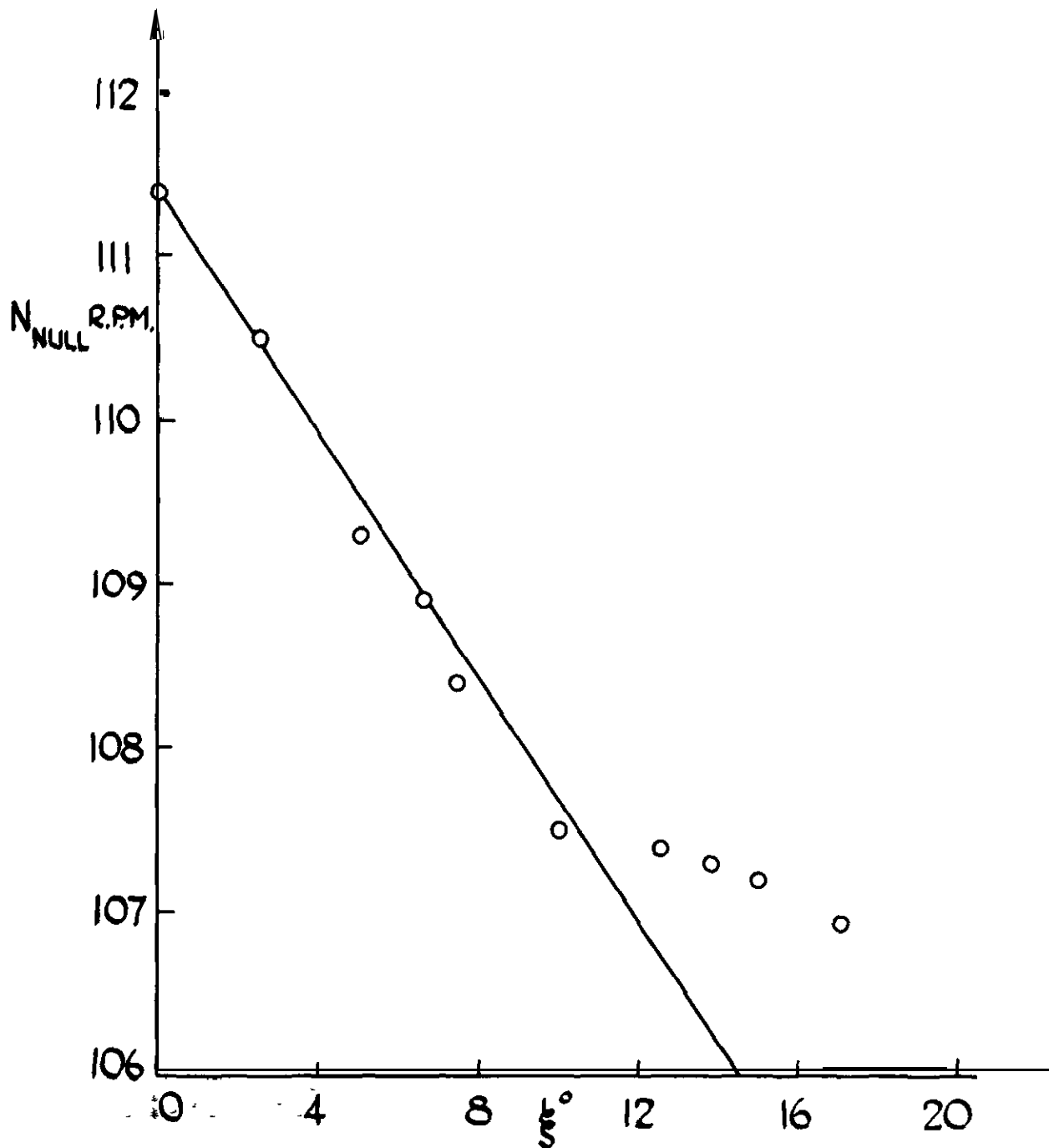
FIG. 11. SPEED TO NULL ROTATING YAWMETER.
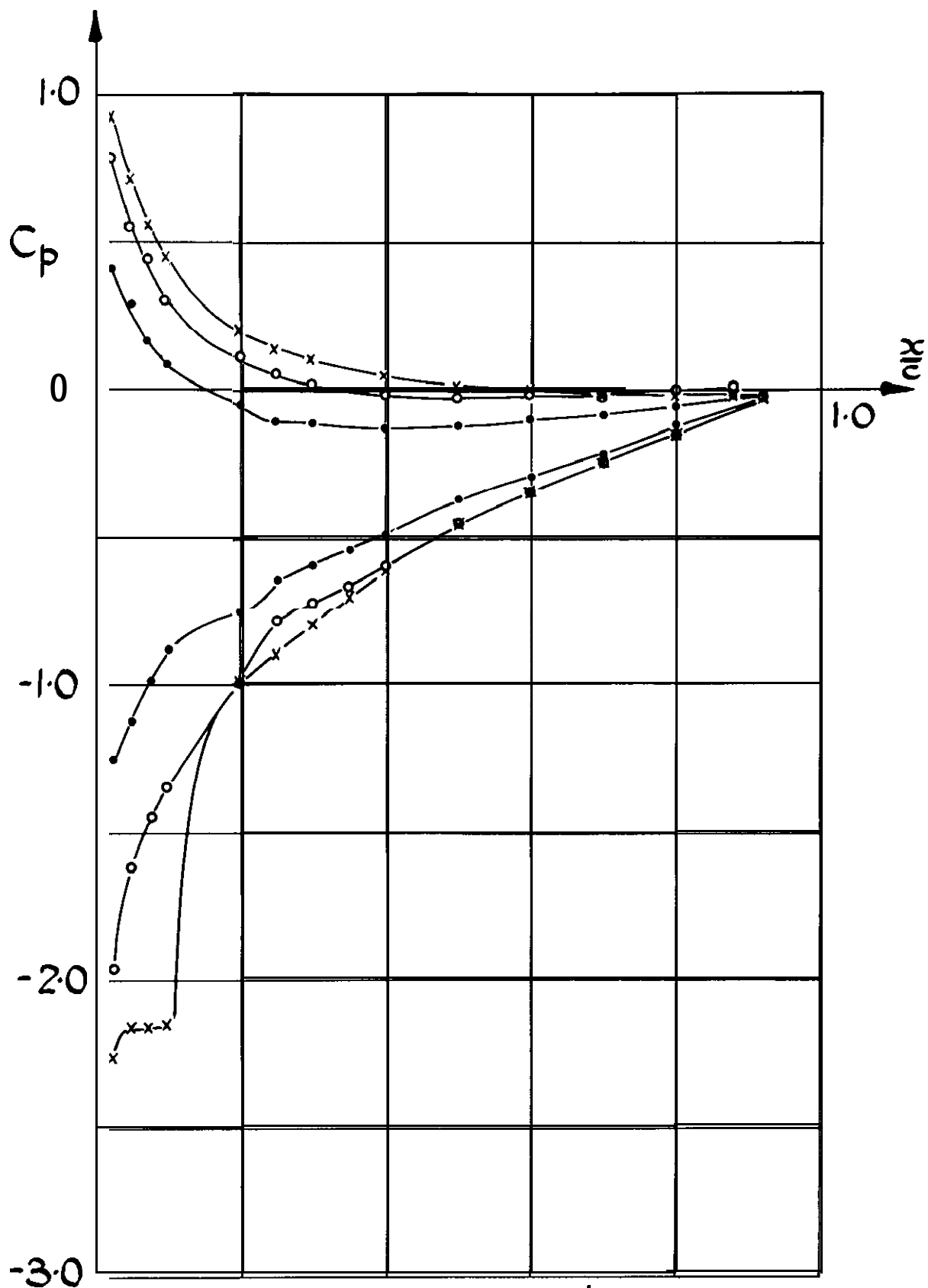
FIG. 12 C_p FOR STATIONARY BLADE.
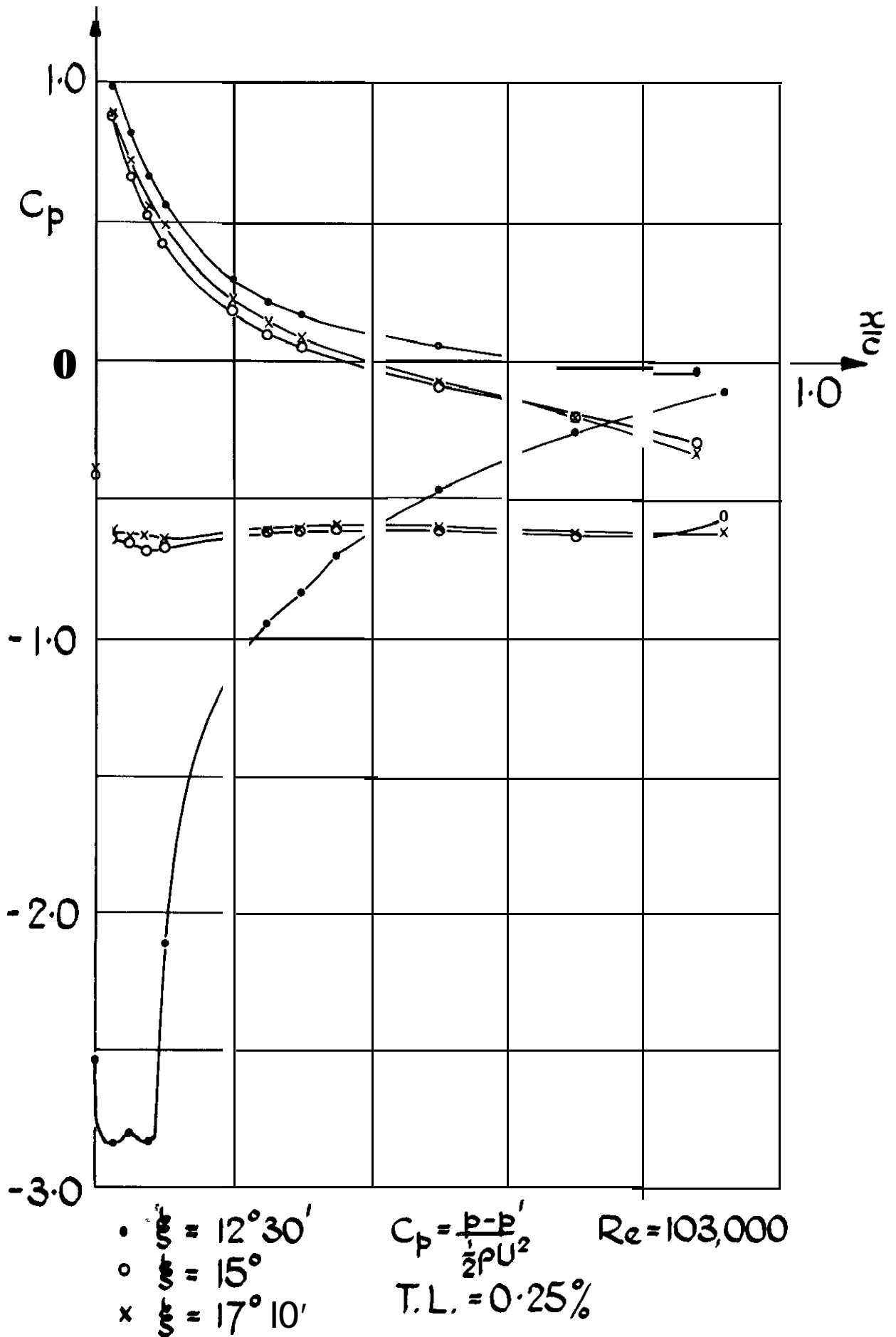
FIG. 13. C_p FOR STATIONARY BLADE

FIG. 14. C_L vs ξ STATIONARY BLADE
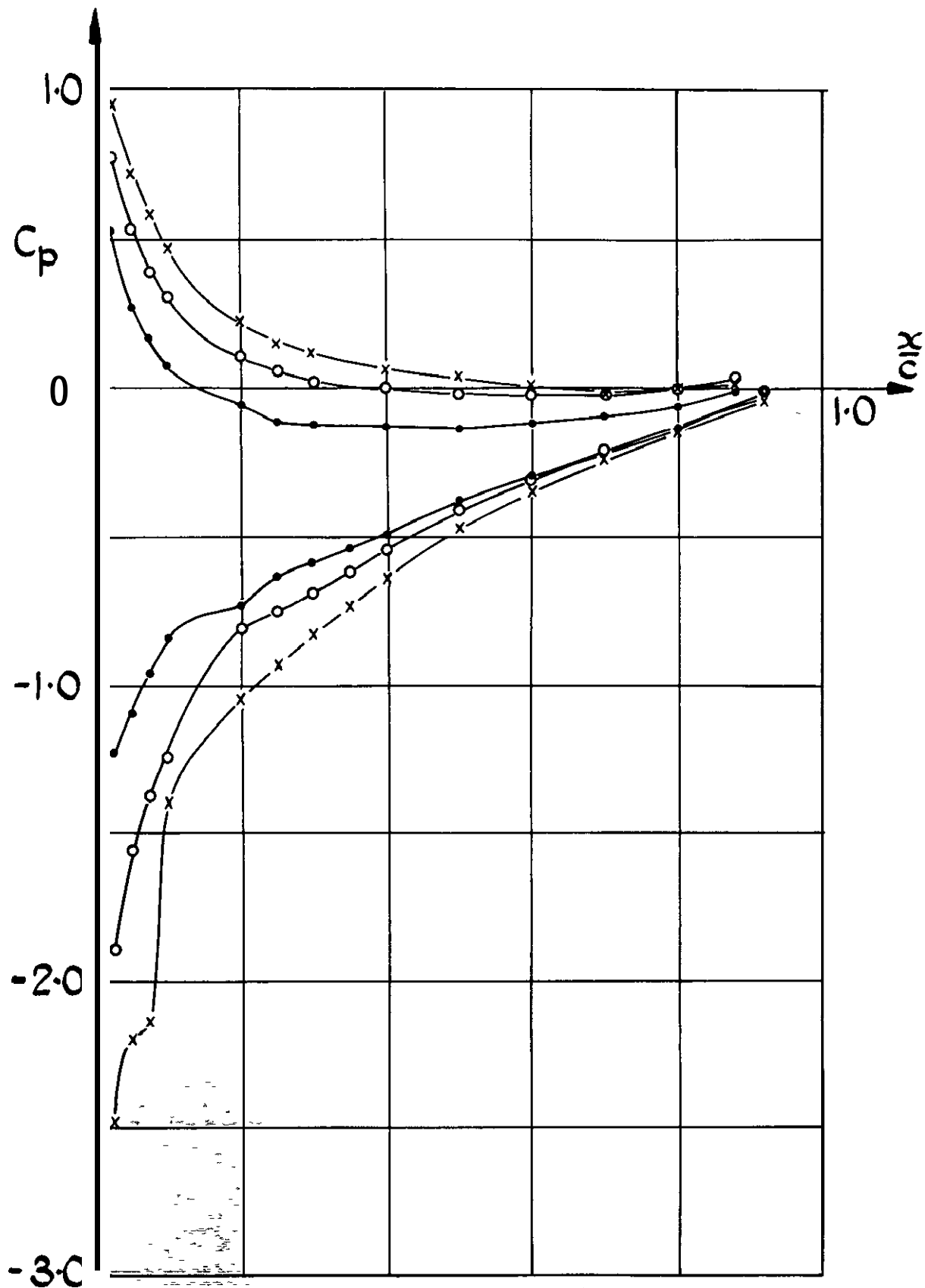
ROTATING T.L. > 1·75%

STATIONARY T.L. = 0·25%

$Re = 103,000$

FIG. 15. C_p FOR STATIONARY BLADE

$\bullet \quad \xi = 5°$

$\circ \quad \xi = 7°30'$

$\times \quad \xi = 10°$
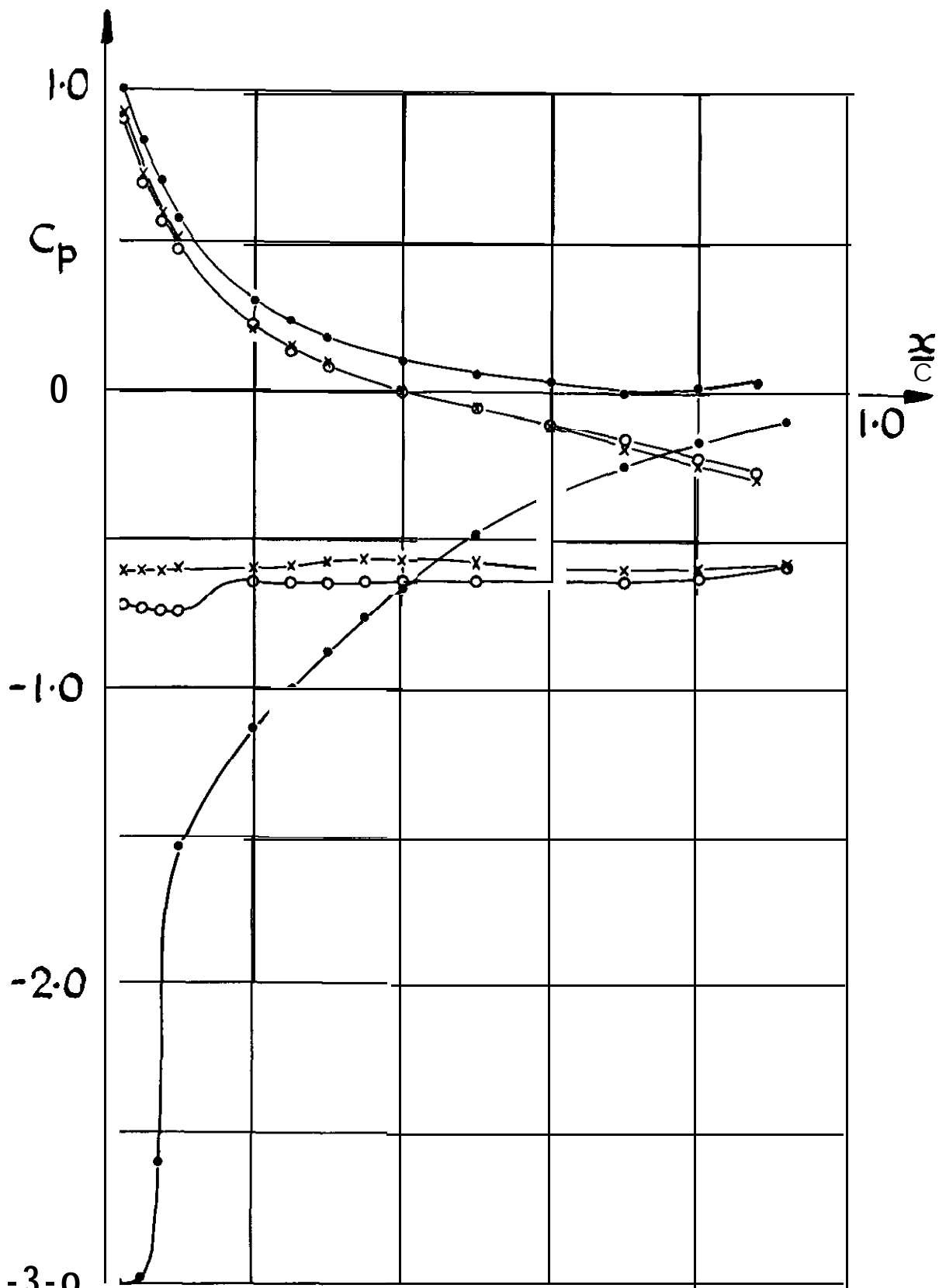
$C_p = \dfrac{p - p'}{\frac{1}{2}\rho U^2} \quad Re = 103,000$

$T.L. = 1.35\%$

FIG. 16. C_p FOR STATIONARY BLADE
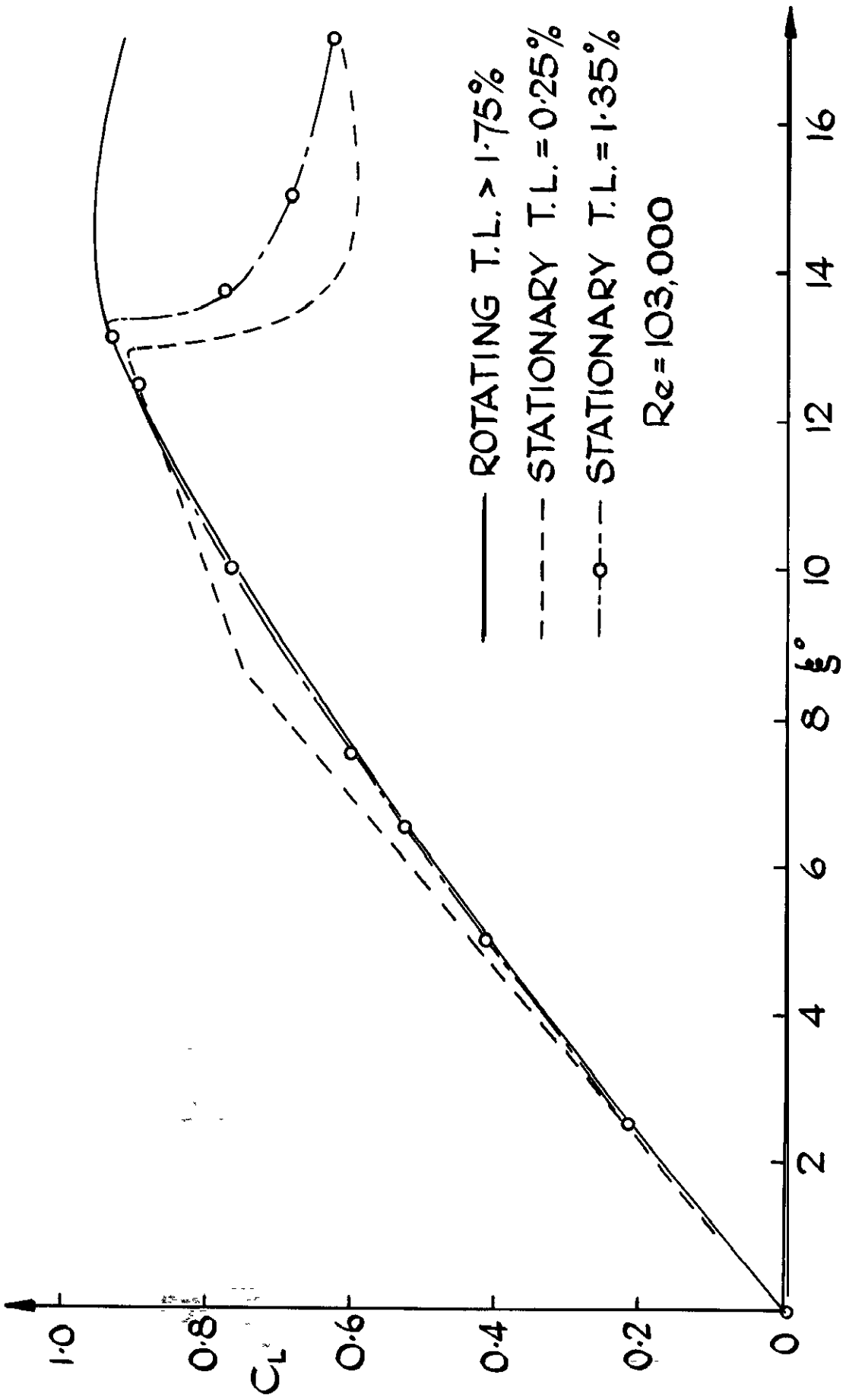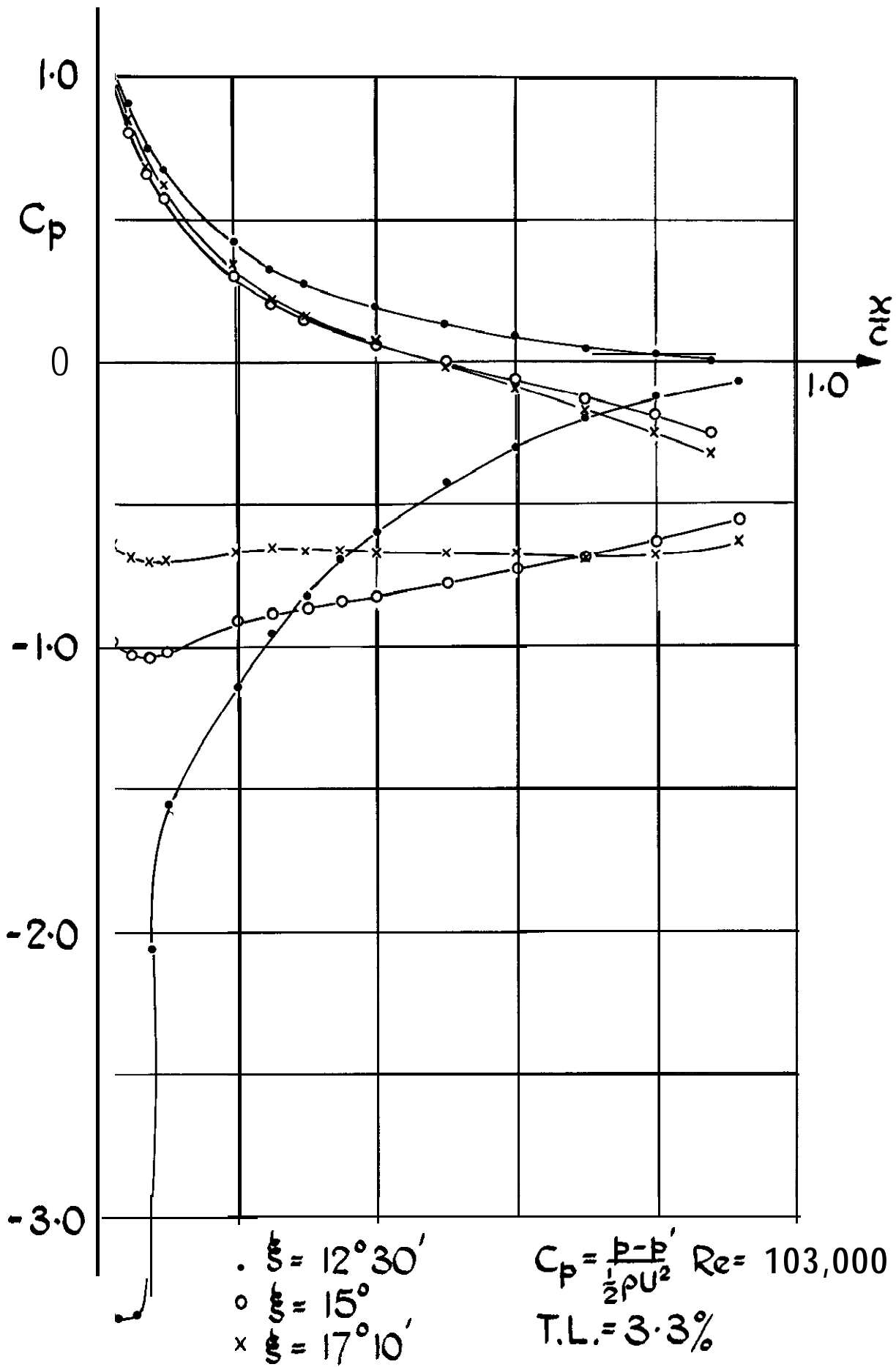
Legend within figure:

• $\xi = 12°30'$

○ $\xi = 15°$

× $\xi = 17°10'$

$C_p = \dfrac{p-p'}{\frac{1}{2}\rho U^2}$ $Re \approx 103,000$

T. L. = 1·35%

FIG. 17. C_L vs ξ STATIONARY BLADE.

ROTATING T.L. > 1·75%

STATIONARY T.L. = 0·25%

STATIONARY T.L. = 1·35%

$R_e = 103,000$

C_L

1·0

0·8

0·6

0·4

0·2

0

2   4   6   8 $\xi°$ 10   12   14   16

FIG. 18. C_p FOR STATIONARY BLADE

Legend (within figure):

$\cdot$ $\xi = 12°30'$

$\circ$ $\xi = 15°$

$\times$ $\xi = 17°10'$

$C_p = \dfrac{p-p'}{\frac{1}{2}\rho U^2}$ $Re = 103,000$

$T.L. = 3.3\%$

Axis labels: C_p (vertical), $\frac{x}{c}$ (horizontal), with values 1.0, 0, -1.0, -2.0, -3.0 on the vertical axis and 1.0 on the horizontal axis.
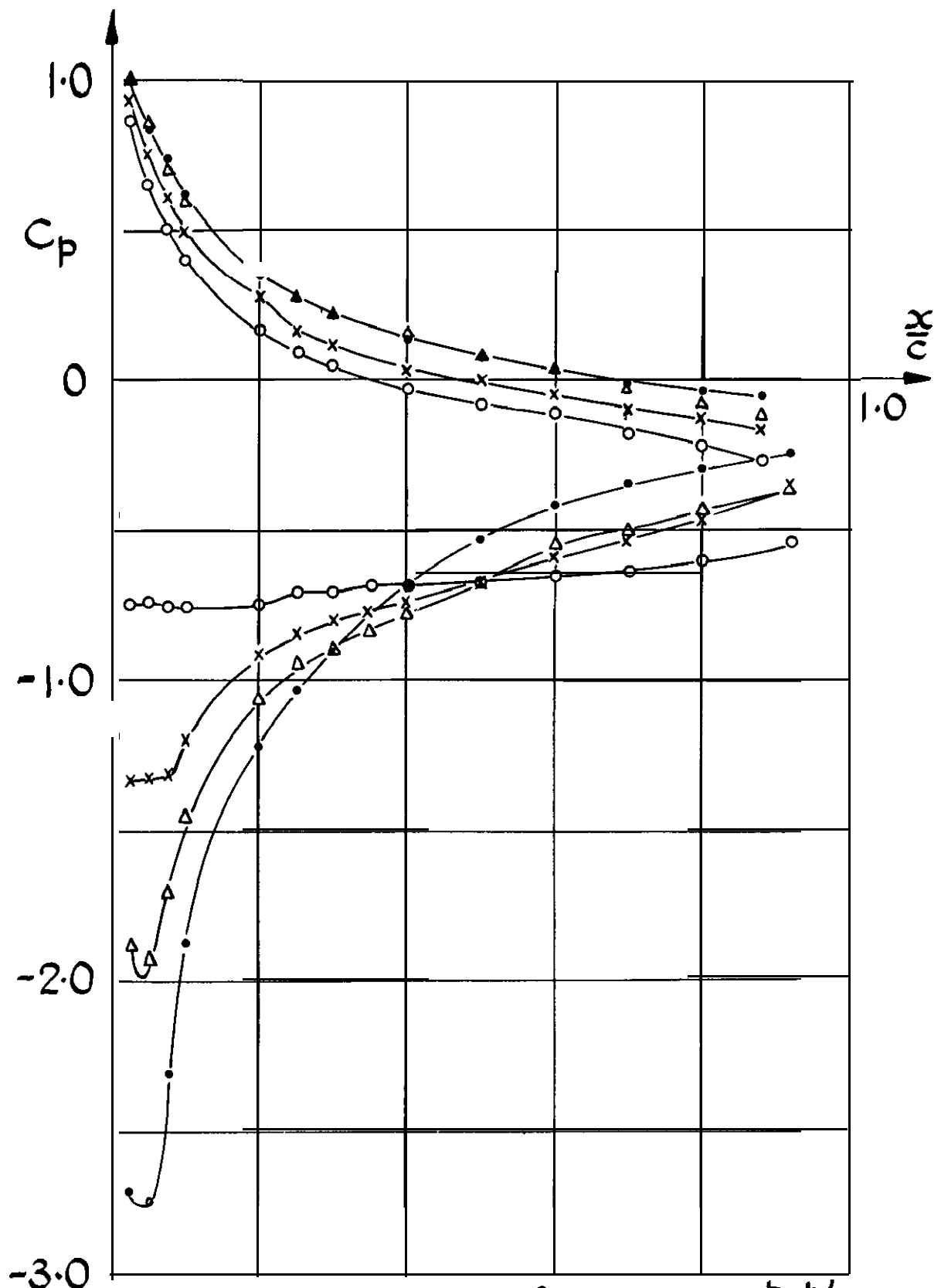
. ROTATING , T. L. >1·75%

○ STATIONARY, T.L.= 0·25%

× STATIONARY. T.l =1·25%

▲ STATIONARY, T.L.= 3·3%

$C_P = \dfrac{p-p'}{\frac{1}{2}\rho U^2}$

$Re = 103,000$
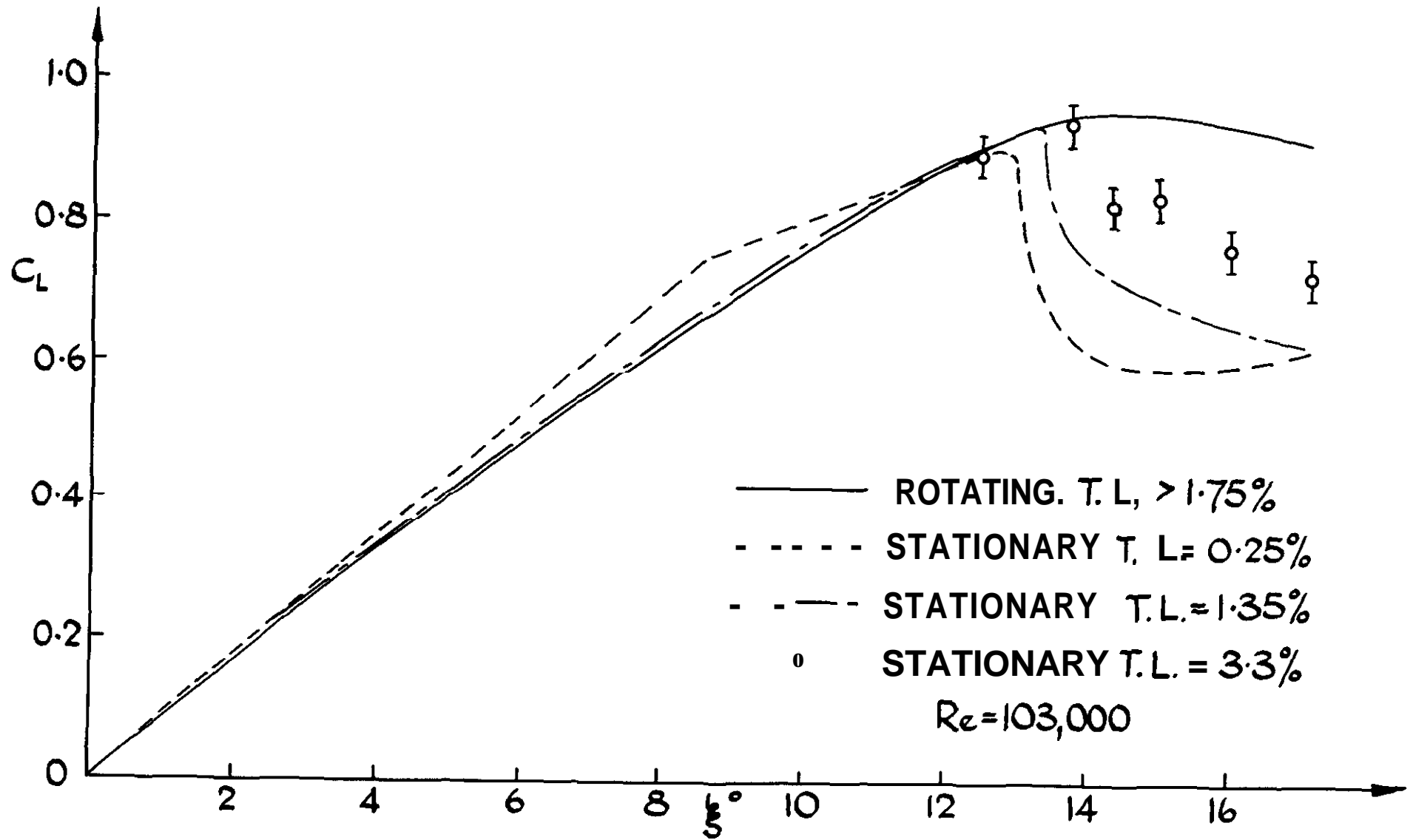
$\xi = 13° 45'$

FIG. 19. THE EFFECT OF TURBULENCE LEVEL.

FIG. 20. C_L vs ξ STATIONARY BLADE